European Journal of Medicinal Chemistry 225 (2021) 113775

Contents lists available at ScienceDirect

European Journal of Medicinal Chemistry

journal homepage: http://www.elsevier.com/locate/ejmech

Design, synthesis and biological evaluation of sphingosine-1-phosphate receptor 2 antagonists as potent 5-FU-resistance reversal agents for the treatment of colorectal cancer

Dongdong Luo [a, 1], Yuhang Zhang [b, d, 1], Shuang Yang [a, 1], Xiaochen Tian [a], Yan Lv [a], Zhikun Guo [c], Xiaochun Liu [a], Gaitian Han [a], Shuai Liu [a], Wenyu Wang [b], Shuxiang Cui [c], Xianjun Qu [b, **], Shengbiao Wan [a, *]

[a] Laboratory for Marine Drugs and Bioproducts of Qingdao National Laboratory for Marine Science and Technology, Key Laboratory of Marine Drugs, Ministry of Education, School of Medicine and Pharmacy, Ocean University of China, Qingdao, 266003, China
[b] Department of Pharmacology, School of Basic Medical Sciences, Capital Medical University, Beijing, 100069, China
[c] Department of Toxicology and Sanitary Chemistry, School of Public Health, Capital Medical University, Beijing, 100069, China
[d] Institute of Clinical Pharmacology, Peking University First Hospital, Beijing, 100034, China

ARTICLE INFO

Article history:
Received 3 June 2021
Received in revised form
27 July 2021
Accepted 11 August 2021
Available online 12 August 2021

Keywords:
S1PR2 antagonists
Colorectal cancer therapy
5-FU-Resistance
Pharmacokinetic properties
Mouse xenograft model

ABSTRACT

5-Fluorouracil (5-FU) and its prodrugs are the essential clinical drugs for colorectal cancer (CRC) treatment. However, the drug resistance of 5-FU has caused high mortality of CRC patients. Thus, it is urgent to develop reversal agents of 5-FU resistance. Sphingosine-1-phosphate receptor 2 (S1PR2) was proved to be a potential target for reversing 5-FU resistance, but the activity of known S1PR2 antagonists JTE-013 were weak in 5-FU-resistant cell lines. To develop more potent S1PR2 antagonists to treat 5-FU-resistant cancer, a series of JTE-013 derivatives were designed and synthesized. The most promising compound **40** could markedly reverse the resistance in 5-FU-resistant HCT116 cells and 5-FU-resistant SW620 cells *via* inhibiting the expression of dihydropyrimidine dehydrogenase (DPD). The key was that compound **40** with improved pharmacokinetic properties significantly increased the inhibitory rate of 5-FU in the SW620/5-FU cells xenograft model with no observable toxicity by inhibiting the expression of DPD in tumor and liver tissues. Altogether, these results suggest that compound **40** may be a promising drug candidate to reverse 5-FU resistance in the treatment of CRC.

1. Introduction

Colorectal cancer (CRC), especially unresectable metastatic colorectal cancer, is one of the most commonly diagnosed cancers with a very high mortality rate [1,2]. Approximately, 1.8 million new cases of CRC and estimated 880,000 deaths worldwide were recorded in 2018 [3]. 5-Fluorouracil (5-FU) and 5-FU pro-drugs are the most essential agents in CRC treatment and the main constituent of therapeutic combinations of multiple cytotoxic agents [4]. 5-FU is converted into 5-fluorouridine-5′-triphosphate (FUTP), 5-fluoro-2′-deoxyuridine-5′-triphosphate (FdUTP), and 5-fluoro-2′-deoxyuridine-5′-monophosphate (FdUMP) *via* interacting with phosphorylated sugars in presence of several enzymes to inhibit thymidylate synthase (TS) activity in cancer cells [5]. Unfortunately, CRC cells could become resistant to 5-FU through multiple mechanisms, and several drug resistance targets have been identified [6–15]. Among all drug resistance mechanisms, 85 % intracellular 5-FU is rapidly degraded into 5,6-dihydro-5-fluorouracil (DHFU) by the over-expressed dihydropyrimidine dehydrogenase (DPD) in cancer cells, ultimately converted to the α-fluoro-β-alanine (FBAL), and excreted *via* the kidneys. This conversion of 5-FU is the main approach by which cancer cells acquire drug resistance [8,15–20]. However, CDHP (gimeracil), the DPD inhibitor in the S-1 regimen, could only inhibit the activity of DPD in the liver, but not in cancer cells [21,22]. Our previous study [23] disclosed that the activation of the downstream signaling (*i.e.* JMJD3) causes increased expression of DPD after the endogenic sphingosine-1-phosphate (S1P) binding with receptor 2 (S1PR2). S1PR2 was identified as a key receptor in

* Corresponding author.
** Corresponding author.
E-mail addresses: quxj@ccmu.edu.cn (X. Qu), biaowan@ouc.edu.cn (S. Wan).
[1] These authors contribute equally to this work.

https://doi.org/10.1016/j.ejmech.2021.113775
0223-5234/

the mechanisms of resistance to 5-FU and targeted inhibition of S1PR2 might be a new avenue to reverse drug resistance of 5-FU. Two classes of S1PR2 antagonists have been reported [24–29] (Fig. 1), and the well-known S1PR2 antagonist JTE-013 have been proved that could effectively reverse 5-FU-resistance and decrease the expression of DPD in 5-FU-resistant HCT116 ($HCT116^{DPD}$) cells. However, our further studies demonstrated that it has weak activity in 5-FU-resistant SW620 (SW620/5-FU) cells. In this study, to further develop efficient S1PR2 antagonists to reverse 5-FU-resistance *in vitro* and *in vivo*, a series of JTE-013 derivatives were synthesized. The surface plasmon resonance (SPR) kinetics of binding to S1PR2 protein of these compounds were investigated, and the changes of refractive index on the chips coated with the protein were measured to estimate ligand binding. The efficacy of synthesized compounds was evaluated in combination with 5-FU in the proliferation of DPD over-expressed and 5-FU-resistant HCT116 ($HCT116^{DPD}$) and 5-FU-resistant SW620 (SW620/5-FU) cells. The inhibitory effects of DPD of these compounds were determined to further investigate their ability to reverse 5-FU resistance. Meanwhile, the most potent compound **40** was also evaluated in nude mouse xenograft models. Our results demonstrate a promising approach to develop a safe and effective treatment of colorectal cancer patients with 5-FU resistance.

2. Results and discussion

2.1. The design strategy of compounds

As illustrated in Fig. 2, based on JTE-013, target compounds were designed in four ways. In the first step, the pyrazolopyridine ring of JTE-013 was changed into pyrrolopyrimidine ring possessed various hydrophobic substituents which are expected to be more potential in the light of our previous studies (for compounds **10**, **14**, and **18**). In the following step, the pyrazolopyridine scaffold was transformed into pyrazolo[1,5-*a*]pyridine with different substituents and the linker was shortened (for compounds **23a-23b** and **25a-25b**). In the next step, the fused ring was changed into a single ring and various hydrophobic substituents were introduced (for compounds **29** and **33**). The final step to gain the target compounds **34**–**40** and **44a-44d** is the replacement of pyrazolopyridine with sing rings bearing various functional groups and shortening of semicarbazide linker.

2.2. Chemistry

Initially, the pyrazolopyridine ring was replaced by pyrrolepyrimidine scaffolds with hydrophobic substituents to afford compounds **10, 14, and 18** (Scheme 1). Intermediates **5** and **12** were synthesized from 2,4-dichloro-1*H*-pyrrolopyrimidine *via* a two-step substitution reaction. Intermediate **16** was synthesized through substitution reaction and Suzuki-Miyaura cross-coupling reaction. Then, compounds **5**, **12**, and **16** reacted with 80 % hydrazine hydrate to produce key intermediates **6**, **13**, **17**. 2,6-dichloro-4-isocyanatopyridine (**9**) was gained from 2,6-dichloropyridine 4-carboxylic acid (**7**) as we reported, and it reacted with compounds **6**, **13**, and **17** to acquire compounds **10**, **14**, and **18**. Subsequently, the linker semicarbazide of JTE-013 was simplified to urea, and its pyrazolopyridine scaffold was transformed into pyrazolo[1,5-*a*]pyridine with different substituents (*i.e.* phenyl and bromine). The ionic type intermediates **21a-21b** were gained from nitriles **20a-20b**, then the cyclization of compounds **21a-21b** under alkaline conditions produced amines **22a-22b**. Compounds **24a** and **24b** were synthesized through Suzuki-Miyaura cross-coupling reaction from compound **22b**, then compounds **23a**, **23b**, **25a**, and **25b** were acquired as similar procedures (Scheme 2). Cyanuric chloride and dichloropyrimidine produced hydrazine compounds **28** and **32** through multistep substitution reaction, then target compounds **29** and **33** were gained (Scheme 3). 2,6-Dichloro-4-isocyanatopyridine (**9**) reacted with different amines to produce urea compounds **34**–**40** (Scheme 4). 2,6-Dichloropyridine 4-carboxylic acid (**7**) reacted with various alcohols to acquire carboxylic acid **41a-41d**. Compounds **41a-41d** were transformed into isocyanates **43a-43d**, which reacted with 2,6-dichloropyridine 4-amide to gain compounds **44a-44d** (Scheme 4).

2.3. Study of binding kinetics of compounds and structure-activity relationships (SAR)

Surface plasmon resonance (SPR) is widely used in studying the interactions of proteins with small molecules. Due to S1PR2 is a class of GPCR proteins, it is difficult to directly study its activity. Thus, an SPR based assay for S1PR2 was established to study the interactions with small molecules. Firstly, the binding ability of compounds was investigated on the S1PR2 protein at 10 μM dose. The results were illustrated as a binding affinity in Table 1. Most compounds showed strong binding abilities (K_D) and the range was from 10 nM to 2 μM. Among them, compounds **23a, 23b, 25a, 25b, 29, 34, 36, 39, 40,** and **44a-44d** showed nanomolar level binding affinity. Especially, the binding affinities of compounds **23a, 23b, 25a, 25b, 34,39,** and **40** were less than 0.1 μM, and the most potent compound **40** showed a strong binding with S1PR2 ($K_D = 13.2$ nM). The above results indicated that these compounds are potent

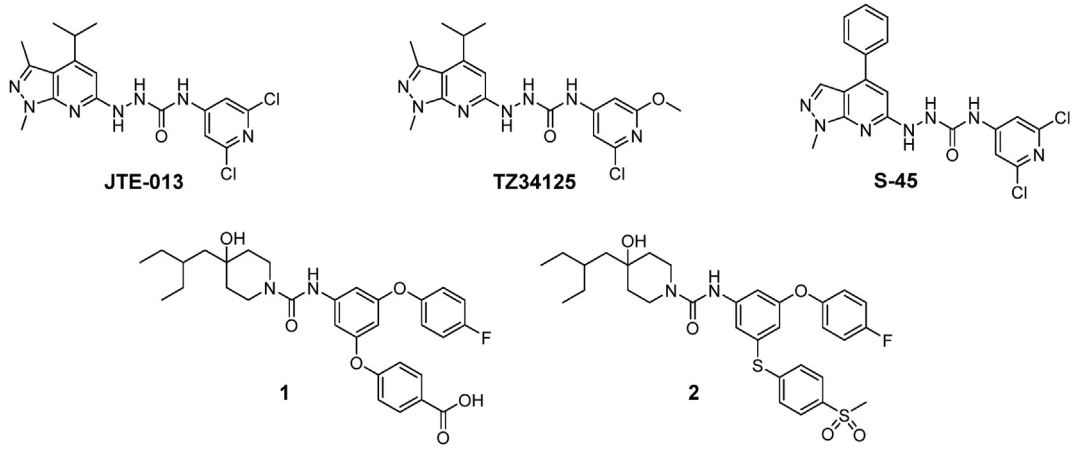

Fig. 1. The structures of reported S1PR2 antagonists.

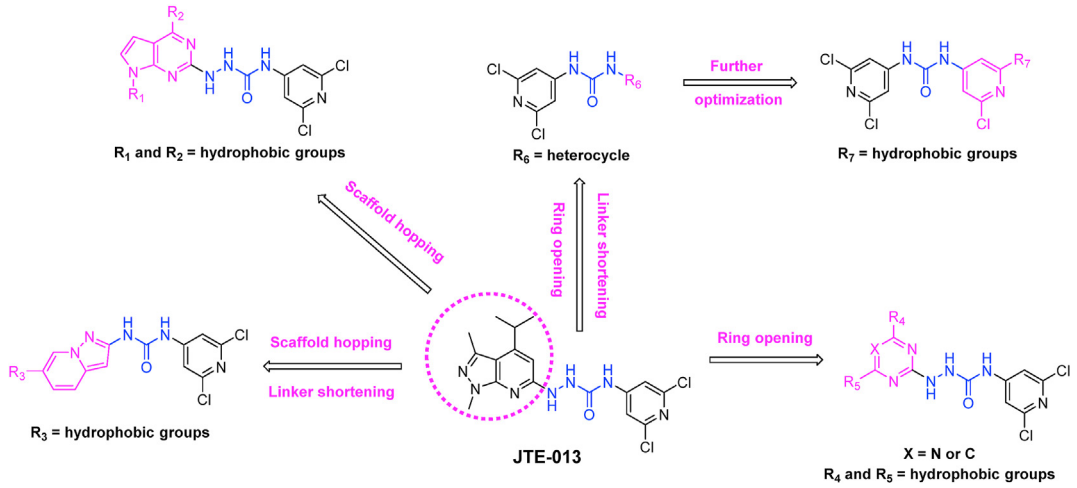

Fig. 2. The design strategy of novel S1PR2 antagonists.

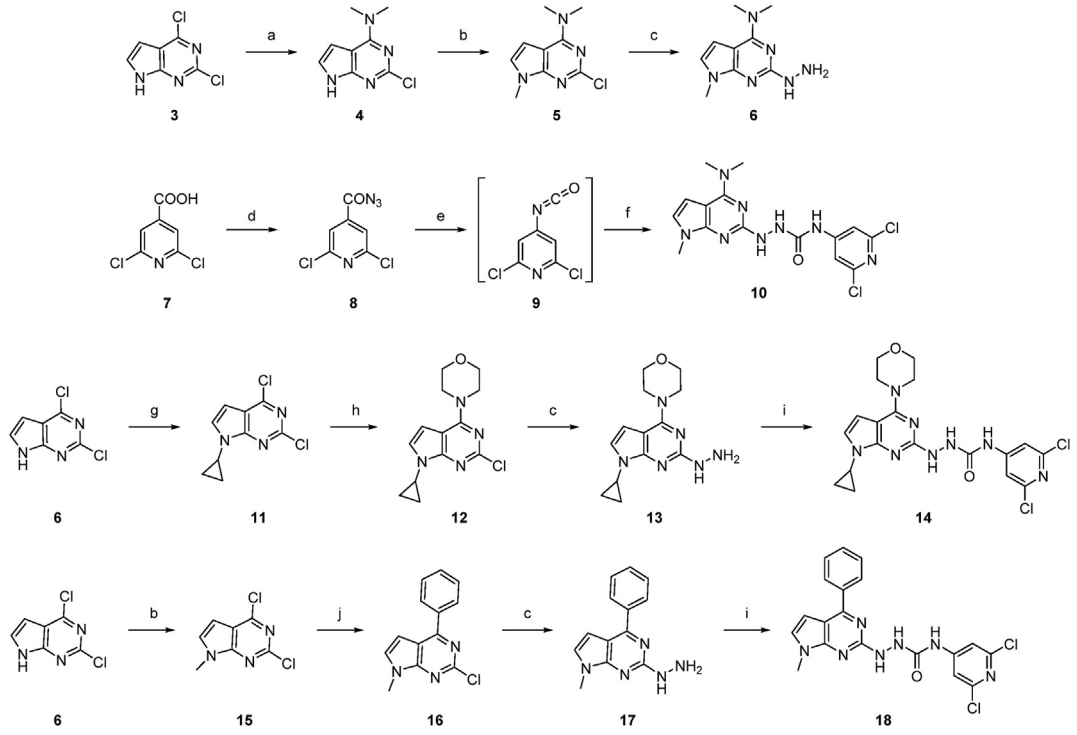

Scheme 1. Synthetic route to compounds **10**, **14**, **18**. Reagents and conditions: (a) $(CH_3)_2NH{\cdot}HCl$, Et_3N, DCM, r.t., overnight, 54 %; (b) CH_3I, NaH, DMF, 0 °C, 2 h, 79–85 %; (c) hydrazine hydrate, EtOH, reflux, 2–3 h, 90–95 %; (d) DPPA, Et_3N, 1,4-dioxane, r.t., 3 h, 67 %; (e) toluene, 80 °C, 2 h; (f) **6**, THF, 50 °C, 12 h, 55 % over two steps; (g) cyclopropylboronic acid, $Cu(OAc)_2$, Na_2CO_3, 2′-2-$(C_5H_4N)_2$, DCM, reflux, 5 h, 45 %; (h) morpholine, Et_3N, DCM, r.t., 5 h, 59 %; (i) toluene, 80 °C, 2 h, then **9**, THF, 50 °C, 12 h, 39–57 % over two steps; (j) phenylboronic acid, $Pd(PPh_3)_4$, Cs_2CO_3, 1,4-dioxane/H_2O, 80 °C, 10 h, 55 %.

antagonists of S1PR2.

2.4. Preliminary biological activities of the compounds against 5-FU-resistant colorectal cancer cell lines via MTT assay and western blotting

To further evaluate the activity of compounds in the 5-FU-resistant colorectal cancer cells, two resistant cell lines ($HCT116^{DPD}$ and SW620/5-FU) were established. The cytotoxic tests showed they are all resistant to 5-FU (IC_{50} > 1000 μM, Fig. S1A), especially SW620/5-FU cells, which were set up by continuously treating with 5-FU. Besides, the levels of DPD protein in $HCT116^{DPD}$ and SW620/5-FU cells were also determined and the results showed that it is dramatically increased relative to parental HCT116 and SW620 cells (Fig. S1B). Initially, compounds combining with 5-FU were screened for their ability to impair the viability of colorectal cancer cells. $HCT116^{DPD}$ and SW620/5-FU cells were concurrently treated with 10 μM 5-FU and 10 μM each of the S1PR2 antagonists for 72 h. Among them, most compounds effectively reduced the cell viability and their inhibition rates were all over 50 % (Fig. S2). In general, not all compounds were as effective in inhibiting SW620/5-FU cells viability as $HCT116^{DPD}$ cells.

Subsequently, all compounds were evaluated for dosage effects on cell proliferation *via* MTT assay. $HCT116^{DPD}$, SW620/5-FU, and

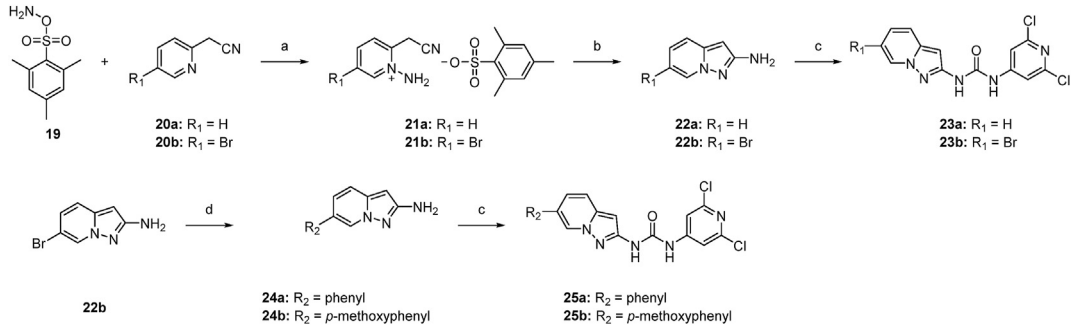

Scheme 2. Synthetic route to compounds **23a-23b**, **25a-25b**. Reagents and conditions: (a) DCM, r.t., 1–3 h, 30–59 %; (b) K_2CO_3, MeOH, r.t., 3 h, 40–67 %; (c) toluene, 80 °C, 2 h, then **9**, THF, 50 °C, 12 h, 39–57 % over two steps; (d) arylboronic acid, $Pd(PPh_3)_4$, Cs_2CO_3, 1,4-dioxane/H_2O, 80 °C, 3 h, 51–59 %.

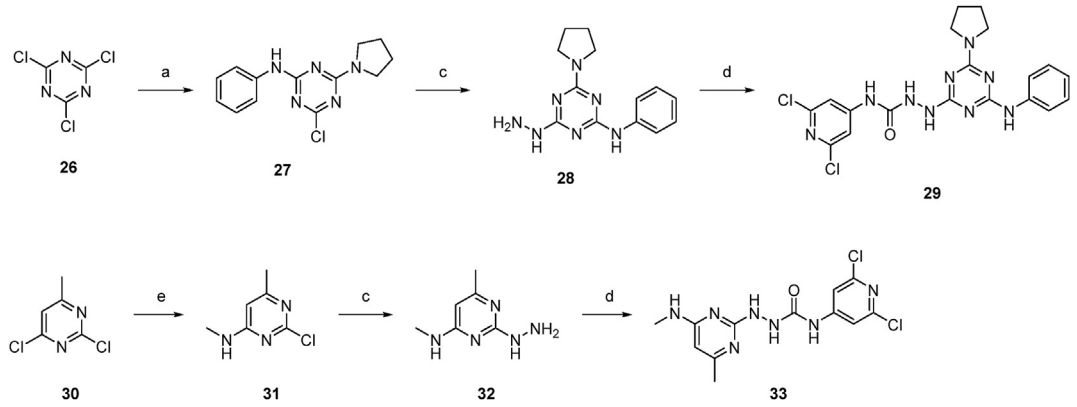

Scheme 3. Synthetic route to compounds **29** and **33**. Reagents and conditions: (a) pyrrole, acetone, 0 °C, 3 h, 60 %; (b) phenylamine, Et_3N, acetonitrile, 0 °C, 5 h, 52 %; (c) hydrazine hydrate, EtOH, reflux, 3 h, 90–95 %; (d) toluene, 80 °C, 2 h, then **9**, THF, 50 °C, 12 h, 55 % over two steps; (e) CH_3NH_2, THF, r.t., overnight, 33 %.

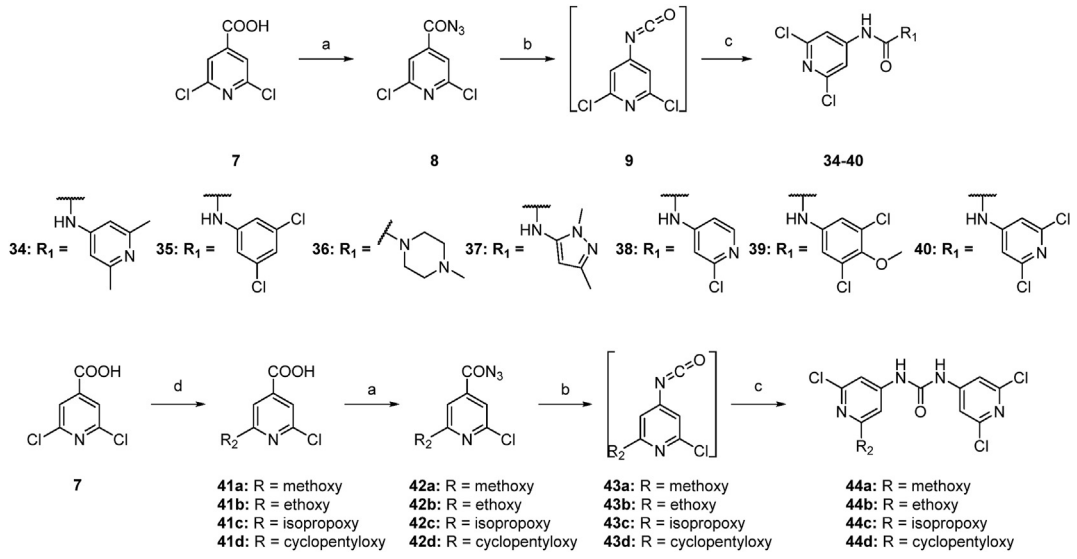

Scheme 4. Synthetic route to compounds **34**–**40** and **44a-44d**. Reagents and conditions: (a) DPPA, Et_3N, 1,4-dioxane, r.t., 3 h, 67 %; (b) toluene, 80 °C, 2 h; (c) amine, THF, 50 °C, 5–15 h, 44–67 % over two steps. (d) alcohol, 1 M NaOH, r.t.-70 °C, 5–12 h, 60–85 %.

NCM460 cells were used as the model system, which were treated with different concentrations of compounds combined with 20 μM 5-FU for 72 h. The values of EC_{50} were calculated and shown in Table 2 and most compounds showed enhanced activity. Compounds **10**, **14**, and **18** possessed pyrrolopyrimidine skeleton all showed no activity to reverse 5-FU-resistance in both resistant cells. Compounds **23a**, **23b**, **25a**, and **25d** all have enhanced 5-FU-resistance reversal activity in both cell lines compared to JTE-013. Remarkably, compound **23a**, being the most potent resistance reversal agent with an EC_{50} value of 2.49 μM against SW620/5-FU cell line. Monocyclic compounds (**29** and **33**) bearing semicarbazide all showed low activity. Surprisingly, monocyclic

Table 1
Kinetics of the interactions between S1PR2 and compounds.

Compds	K_a ($M^{-1}s^{-1}$)	K_d (s^{-1})	K_D (M)
JTE-013	8.21×10^4	1.61×10^{-1}	1.96×10^{-6}
10	7.55×10^4	1.02×10^{-1}	1.85×10^{-6}
14	6.12×10^4	1.33×10^{-1}	2.17×10^{-6}
18	5.21×10^4	1.36×10^{-1}	2.61×10^{-6}
23a	7.93×10^6	1.16×10^{-1}	1.46×10^{-8}
23b	8.31×10^7	1.68	2.02×10^{-8}
25a	4.59×10^6	2.01×10^{-1}	4.38×10^{-8}
25b	9.12×10^6	1.12×10^{-1}	1.22×10^{-8}
29	7.15×10^5	1.33×10^{-1}	1.86×10^{-7}
33	5.56×10^4	2.36×10^{-1}	4.24×10^{-6}
34	5.69×10^6	1.46×10^{-1}	2.57×10^{-8}
35	3.26×10^4	1.16×10^{-1}	3.56×10^{-6}
36	1.98×10^5	1.06×10^{-1}	5.35×10^{-7}
37	5.36×10^4	1.77×10^{-1}	3.30×10^{-6}
38	3.65×10^4	2.01×10^{-1}	5.50×10^{-6}
39	6.24×10^6	3.12×10^{-1}	5.00×10^{-8}
40	5.28×10^6	6.97×10^{-1}	1.32×10^{-8}
44a	3.21×10^5	2.19×10^{-1}	6.82×10^{-7}
44b	1.96×10^5	1.02×10^{-1}	5.20×10^{-7}
44c	9.14×10^5	1.19×10^{-1}	1.30×10^{-7}
44d	4.49×10^5	1.79×10^{-1}	3.99×10^{-7}

K_a, association constant; K_d, dissociation constant; $K_D = K_d/K_a$.

Table 2
In vitro antiproliferative efficacy of synthetic compounds in three cell lines.

Compds	EC_{50} (μM)		
	SW620/5-FU	$HCT116^{DPD}$	NCM460
JTE-013	58.58 ± 1.21	17.13 ± 1.25	61.34 ± 1.78
10	48.25 ± 1.57	41.50 ± 0.73	58.53 ± 0.57
14	436.27 ± 34.74	449.27 ± 41.74	549.21 ± 11.33
18	528.12 ± 13.52	660.12 ± 29.52	683.23 ± 45.21
23a	2.49 ± 0.26	5.13 ± 0.41	10.23 ± 2.15
23b	11.72 ± 1.56	5.26 ± 0.87	8.94 ± 0.92
25a	9.25 ± 0.52	5.13 ± 0.33	8.05 ± 0.37
25b	9.62 ± 1.82	5.35 ± 0.19	8.35 ± 1.78
29	31.95 ± 1.42	23.16 ± 0.93	65.23 ± 4.32
33	122.24 ± 2.72	23.40 ± 1.54	65.26 ± 0.89
34	234.14 ± 1.72	86.21 ± 0.34	576.34 ± 2.13
35	12.24 ± 0.72	11.40 ± 1.54	55.42 ± 0.89
36	548.25 ± 1.57	141.50 ± 7.73	521.13 ± 1.25
37	67.21 ± 1.81	94.21 ± 3.25	134.21 ± 1.23
38	31.15 ± 1.37	16.13 ± 1.78	55.34 ± 1.61
39	8.25 ± 1.57	41.50 ± 0.73	27.32 ± 0.55
40	0.21 ± 0.03	0.18 ± 0.04	9.44 ± 0.13
44a	14.21 ± 1.01	11.18 ± 0.65	33.21 ± 0.53
44b	8.15 ± 0.37	6.13 ± 0.78	25.34 ± 0.51
44c	5.17 ± 0.12	5.23 ± 0.56	21.12 ± 3.15
44d	6.15 ± 1.43	5.12 ± 0.97	21.43 ± 2.12
5-FU[a]	>1000	>1000	43.32 ± 1.98

Data are presented as mean ± SD at least three independent experiments and the concentration of 5-FU is 20 μM.
[a] The value of EC_{50} (5-FU) is the median inhibitory concentration of single 5-FU against three cell lines.

compounds containing chlorinated aromatic ring showed potent activity in both resistant cells, which indicated that chlorine atom may be the key to increase activity. Most notably, compound **40** possessing four chlorine atoms showed nanomolar level activity in both resistance cells, and there are a 95-fold improvement in potency against $HCT116^{DPD}$ cells (0.18 μM) and a 279-fold improvement against SW620/5-FU cells (0.21 μM) compared with JTE-013. More importantly, it showed obvious selectivity towards normal NCM460 cells (9.44 μM). Although compounds **44a-44d** also showed potent activity (EC_{50} < 10 μM) to reverse 5-FU-resistance compared with JTE-013, but there are reductions of activity compared with compound **40**. These results further showed the importance of the chlorine atom. In addition, compounds with well 5-FU-resistance reversal activity (**23a, 23b, 25a, 25b, 35, 39, 40, 44a-44d**) were selected to test the ability to down-regulate DPD in SW620/5-FU cells by western blotting and they all showed strong activity to inhibit the expression of DPD (Fig. S2B). Among them, compound **40** showed the strongest activity and deserved further exploration.

2.5. Compound *40* inhibited the expressions of DPD and JMJD3 to reverse 5-FU resistance

The efficacy of compound **40** to down-regulate the expression of DPD was tested at low concentrations in $HCT116^{DPD}$ and SW620/5-FU cells. Compound **40** could suppress the expression of DPD in a dose-dependent manner (Fig. 3). Moreover, our previous study ascertained that **S-45** and JTE-013 could effectively restrain 5-FU-induced S1PR2 internalization into the endoplasmic reticulum (ER) and inhibit the expression of JMJD3. Enlightened from our previous discoveries, the JMJD3 was also tested and it was found that compound **40** effectively restrained the expression of JMJD3 (Fig. 3). S1PR2 was reported with multiple biological effects *in vivo* and its decrease in expression level may cause unexpected side effects. Therefore, it was important to assess whether compound **40** could affect the expression of S1PR2 to reduce the expression of DPD. $HCT116^{DPD}$ and SW620/5-FU cells were used to explore the effect of compound **40** on the expression of S1PR2 at different concentrations. The data clearly showed that the expression of S1PR2 was hardly affected by compound **40** (Fig. 3). Overall, the above data demonstrated that compound **40** had more potential to reverse 5-FU resistance in 5-FU-resistant colorectal cancer cell lines compared with JTE-013.

2.6. Compound *40* increase intracellular concentration of 5-FU to reduce the dosage of 5-FU

Intracellular 5-FU could be rapidly degraded by intracellular DPD and to further verify whether compound **40** could prohibit the reduction of intracellular concentration of 5-FU or not, we determined to test intracellular 5-FU levels in SW620/5-FU cells after treatments with compound **40** and 5-FU. As expected, the HPLC analysis demonstrated that the degradation of intracellular 5-FU was hindered by compound **40** and JTE-013, which could increase the concentration of 5-FU from 0.59 mg/L to 10.01 mg/L and 4.87 mg/L, respectively (Fig. 4A). The decrease levels of FBAL were consistent with the degradation levels of 5-FU, which showed 0.17 mg/L and 1.37 mg/L FBAL in compound **40** and JTE-013 treated SW620/5-FU cells compared with 2.88 mg/L FBAL in control SW620/5-FU cells. These results suggested that compound **40** could prevent the degradation of 5-FU into FBAL and significantly increase the intracellular concentration of 5-FU in 5-FU-resistant colorectal cancer cells. To further evaluate the activity of compound **40**, SW620/5-FU cells were treated with compound **40** and the inhibitory effects of different concentrations of 5-FU were tested. It was found that the increased dosage of compound **40** could effectively reduce the dosage of 5-FU to achieve the same inhibition rate in SW620/5-FU cells (Fig. 4B).

2.7. Binding models for compound *40* in the S1PR2-binding pocket

It is reported that an allosteric site of S1PR2 was found close to the orthosteric binding site [30]. Considering biological data of compound **40**, it was proposed that compound **40** may not bind to the orthosteric binding site. The allosteric site was inferred (Fig. 5A) and compound **40** was docked *in silico* into the allosteric binding pocket to explore the differences of the binding modes between compound **40** and JTE-013. Based on the known interactions, the

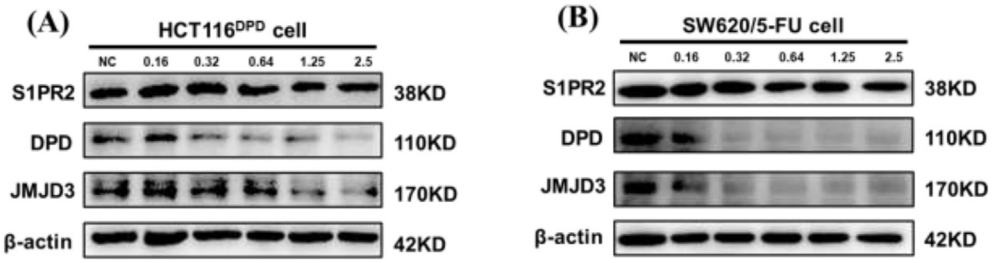

Fig. 3. Compound **40** reversed 5-FU resistance by inhibiting the expression of intracellular DPD. (A) The expressions of S1PR2, DPD, JMJD3 in HCT116^{DPD} cells were determined after treatments with compound **40**. (B) The expressions of S1PR2, DPD, JMJD3 in SW620/5-FU cells were determined after treatments with compound **40**.

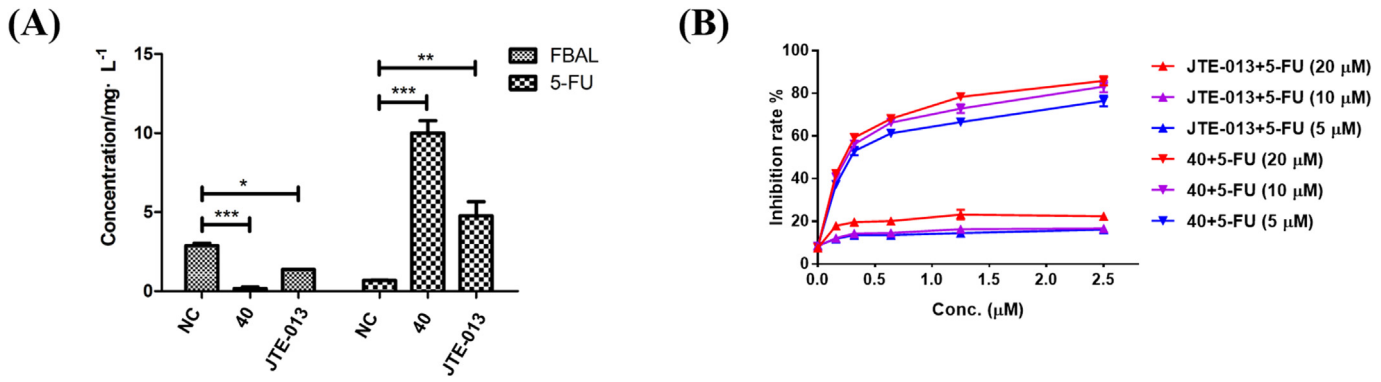

Fig. 4. Compound **40** reversed 5-FU resistance by reducing DPD-catalyzed degradation of intracellular 5-FU. (A) HPLC analysis of intracellular 5-FU and FBAL in SW620/5-FU cells after treatments with 5-FU combined with compound **40** or JTE-013. (B) The inhibition rates of dose-gradient compound **40** and JTE-013 were measured in SW620/5-FU cells after treatments with 20, 10, and 5 μM 5-FU. Data are presented as mean ± SEM. $*p < 0.05$, $**p < 0.01$ and $***p < 0.001$.

final ligand-receptor complexes were ranked according to the docking score. With the docking results, we observed that JTE-013 interacts with Tyr18, Arg108, Glu109, and Val182 by hydrogen bonds. The hydrocarbon alkyl and dichloropyridine tail are in the

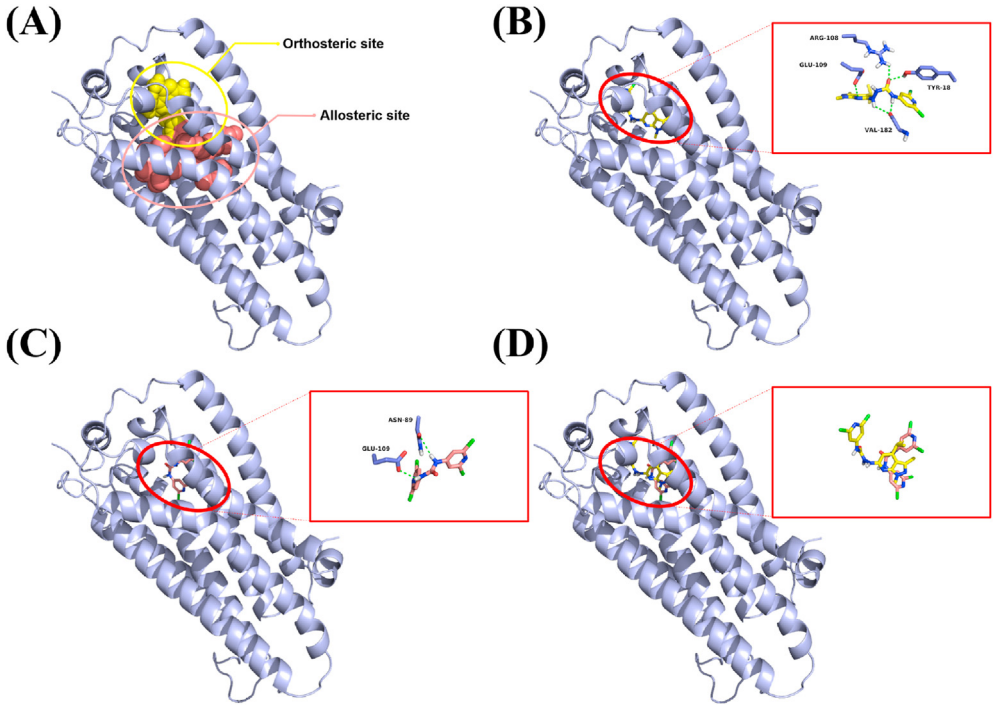

Fig. 5. Molecular docking studies. (A) The homology model of human S1PR2 (light blue ribbons) from the crystal complex of S1PR1 (PDB ID: 3V2Y) and the putative orthosteric binding sites (cyan sphere) and allosteric binding sites (carmine sphere). (B) Docked result of JTE-013 (yellow carbon sticks) at the orthosteric site and specific amino acid residues. (C) Docked result of compound **40** (carmine carbon sticks) at the allosteric site and specific amino acid residues. (D) superposition of JTE-013 binding mode and compound **40** binding modes in S1PR2. Atom color code: oxygen = red, nitrogen = blue, hydrogen = white, chlorine = green. Hydrogen bonds are indicated by green dashed lines.

hydrophobic pocket (Fig. 5B). Compound **40** occupies another hydrophobic pocket and interacts with Asn89 by apparent hydrogen bonds (Fig. 5C). Co-docking of JTE-013 and compound **40** suggested that the receptor pocket could accommodate JTE-013 in the hydrophobic pocket close to the surface of the protein, while compound **40** could reach the interior part of the protein (Fig. 5D). The binding mode between **40** and S1PR2 reasonably explained the 5-FU resistance reversal activities of compound **40** in $HCT116^{DPD}$ and SW620/5-FU cells.

2.8. Pharmacokinetic profile of compound *40*

The pharmacokinetic profile of compound **40** and JTE-013 were examined in *in vivo* and *in vitro*. The amount of compound **40** was no changed significantly in the incubation of MLM and RLMs with NADPH generation for the 97.9 % and 95.2 % remaining after 60 min incubation. Mean plasma and blood concentration of compound **40** and JTE-013 versus time profiles are illustrated (Fig. 6), while mean major pharmacokinetic parameters are presented in Table 3. The concentration of compound **40** at all collection time points was lower in whole blood than plasma. The concentration at time zero (C_0) and area under the concentration curve (AUC) of compound **40** in plasma were about 2-fold of those in whole blood. Meanwhile, the elimination half-life ($t_{1/2}$) and mean residence time (MRT) of compound **40** were similar in whole blood (4.4 h) and plasma (4.7 h). However, JTE-013 plasma and blood concentrations at 8 h after dosing and beyond were below the limit of quantification (LOQ, 1 ng/mL). The AUC of JTE-013 in whole blood was higher than in plasma. In addition, the clearance of compound **40** was significantly lower than JTE-013. Moreover, compound **40** and JTE-013 between whole blood and plasma appear strongly correlated with Pearson's correlation coefficients of 0.9765 and 0.9313, respectively. The median whole blood to plasma ratios measured at all collection time points were 0.484 (0.285–0.671) for compound **40**, which differs significantly ($p < 0.001$) from JTE-013 with the median ratio of 1.622 (0.859–3.442). It was suggested that there was no binding between **40** and hemocytes, meanwhile, JTE-013 has an affinity to the blood cells.

2.9. Compound *40* combined with 5-FU suppresses tumor growth in SW620/5-FU xenograft mice

To evaluate the 5-FU resistance reversal activity of compounds **40** *in vivo*, the SW620/5-FU xenograft model was established. The mice were treated intravenously with the combination of 5-FU (20 mg/kg/day) and compound **40** (1.08 mg/kg/day) for consecutive 24 days. The combination of 5-FU (20 mg/kg/day) and JTE-013 (12.50 mg/kg/day) was used as a positive control. The body weights of mice in the 5-FU plus compound **40** group continuously leveled off, whereas body weights in the positive control group continued to lose weight after 12 days (Fig. 7A). The mice treated with 5-FU plus compound **40** showed a significant effect on inhibiting tumor growth and the inhibition rate increased from 18.54 % to 66.16 % compared with those treated with 5-FU alone (Fig. 7B–D). In contrast, the effect of JTE-013 was not as effective as compound **40** and the inhibition rate of JTE-013 plus 5-FU was only 29.88 % (Fig. 7D). Besides, the treatment with compound **40** alone hardly inhibited the tumor growth with the inhibition rate of 7.50 % (Fig. 7D).

In addition, to verify whether compound **40** could prevent DPD expression *in vivo*, DPD expression levels in liver, colon, and tumor of nude mice were also measured. The results of western blotting suggested that compound **40** could largely inhibit DPD expression in tumor and liver tissues (Fig. 8A). Immunohistochemistry assays were also performed in the paraffin-embedded tumor and tissue sections, and the staining of the tumor and liver showed that compound **40** and JTE-013 strongly inhibited DPD expression in the tumoral and liver specimens with no observable toxicities. The scattered staining was demonstrated in colonic tissues, while DPD staining was impaired by compound **40** but not JTE-013 (Fig. 8B). These results suggested that compound **40** could effectively reverse 5-FU resistance through inhibiting DPD expression *in vivo*.

Table 3
Pharmacokinetic parameters for **40** and JTE-013 in blood and plasma after a single intravenous injection at 1 mg/kg in rats (n = 3)[a].

Parameter	40		JTE-013	
	Blood	Plasma	Blood	Plasma
C_0 (ng/mL)	489.1	1110.1	1838.9	2020.1
$t_{1/2}$ (h)	4.4	4.7	1.0	1.1
$AUC_{(0-t)}$ (h ng/mL)	1894.6	3838.2	725.9	481.7
$AUC_{(0-\infty)}$ (h ng/mL)	1947.7	3956.8	737.8	484.0
V_d (L/kg)	3.3	1.7	2.1	3.1
CL (L/h/kg)	0.51	0.25	1.4	2.1
$MRT_{(0-t)}$ (h)	6.0	6.2	0.9	0.9
$MRT_{(0-\infty)}$ (h)	6.7	7.0	1.0	0.9

[a] C_0, concentration at time zero after intravenous dose; $t_{1/2}$, half-life; AUC, area under the concentration curve; V_d, apparent volume of distribution; CL, clearance; MRT, mean residence time.

3. Conclusions

5-FU, the earliest antimetabolites for cancer therapy, has been widely used in the therapy of various solid tumors, especially gastrointestinal tumors. Yet, the emergence of drug resistance has greatly limited its applications. Cancer cells could develop 5-FU resistance through overexpression of DPD, which is the main enzyme to degrade 5-FU. Our previous study revealed that S1PR2 up-regulated the expression of DPD to accelerate the degradation of intracellular 5-FU, and S1PR2 inhibition could overcome resistance

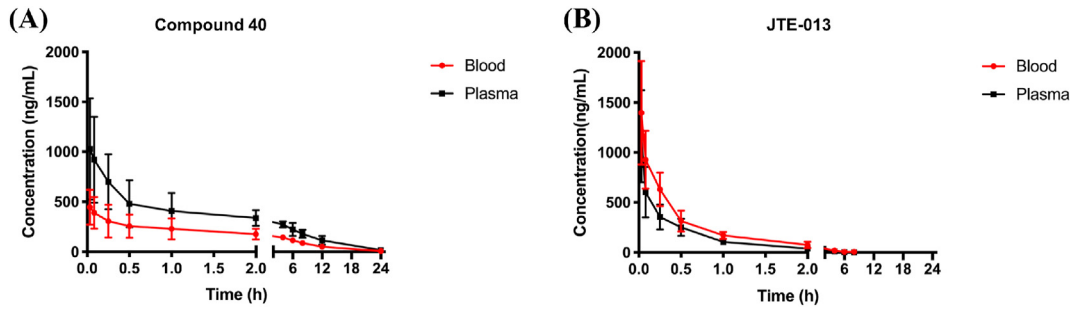

Fig. 6. Mean concentration-time curves in plasma (black line) and whole blood (red line) after intravenous injection of **40** and JTE-013 at 1 mg/kg in mice (n = 3).

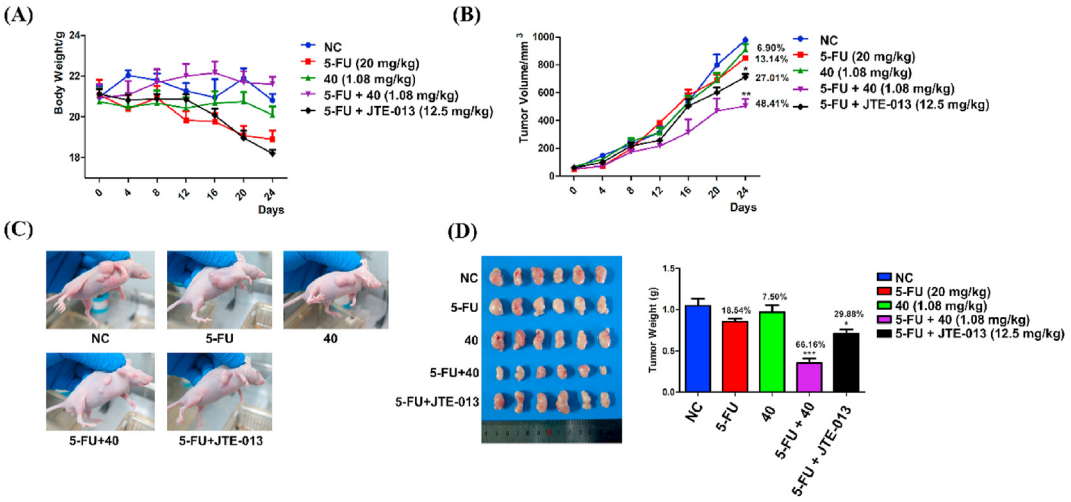

Fig. 7. The inhibitory effects of compound **40** combined with 5-FU in the SW620/5-FU xenografted athymic mice, n = 6. (A) Body weight changes of mice were measured every four days during treatment. (B) Tumor volume changes of mice were measured every four days during treatment. (C) Representative tumor-bearing nude mice of every group. (D) Picture of dissected SW620/5-FU tumor tissues of each group. Data are presented as mean ± SEM. $*p < 0.05$, $**p < 0.01$ and $***p < 0.001$.

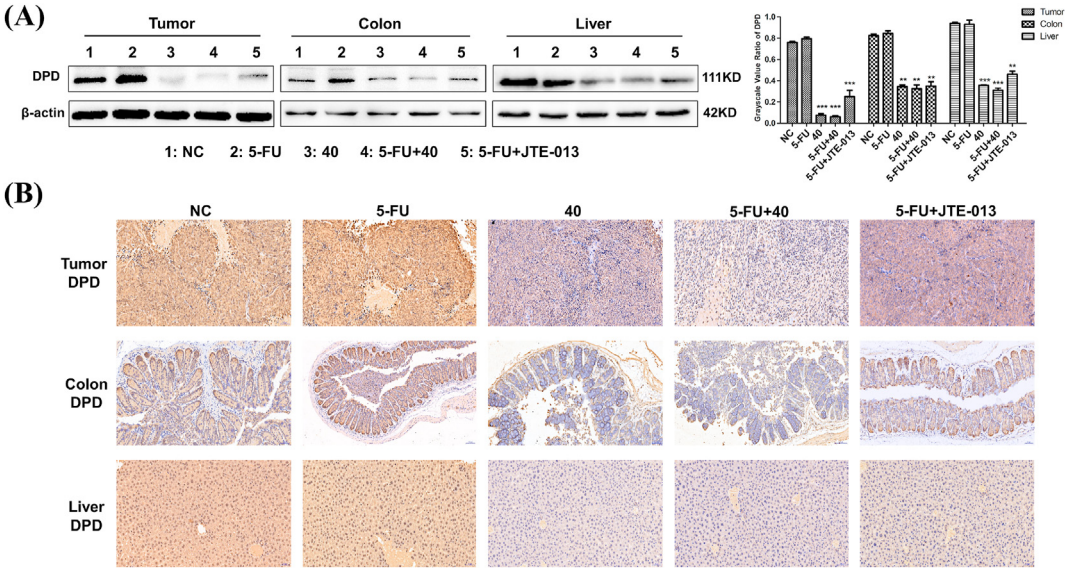

Fig. 8. Compound **40** prevented 5-FU resistance *in vivo* by downregulating DPD expression, n = 6. (A) DPD expressions were analyzed in tumor and various tissues. Histogram showed the ratios of their corresponding grayscale values to β-actin in the right panel. (B) DPD expressions were analyzed in tumor and various tissues of each group by immunohistochemistry. Data are presented as mean ± SEM. $*p < 0.05$, $**p < 0.01$ and $***p < 0.001$.

via reducing intracellular DPD. The previously identified S1PR2 antagonist **S-45** has excellent *in vitro* activity compared with JTE-013, but its *in vivo* activity was unsatisfactory.

In this study, using a structure-based approach, we designed and synthesized novel small molecules that effectively inhibited S1PR2, with verified effects *in vitro* and *in vivo*. The initial screening included $HCT116^{DPD}$ cells, SW620/5-FU cells, and non-cancerous Colonic NCM460 cells *via* MTT assay. Among all compounds, compound **40** was selected for further investigations due to its superior activity to reverse 5-FU resistance and inhibit DPD expression, and reasonably good selectivity. Furthermore, compound **40** was analyzed for its ability to decrease the dosage of 5-FU and inhibit the JMJD3-H3K27me3-DPD pathway in 5-FU-resistant colorectal cancer cells. And it was found that compound **40** could reduce the use of 5-FU and suppress the expression of JMJD3 in a concentration-dependent manner. Further HPLC analysis showed that compound **40** could prevent the degradation of 5-FU into FBAL in cells. More importantly, the 5-FU resistance reversal activity of compound **40** was verified in the colorectal cancer xenograft mouse model. The combination of compound **40** and 5-FU significantly inhibited tumor growth and decreased tumor weight by 66.16 %, which was greater than that of the control group (JTE-013 and 5-FU group). Concurrently, the treatment with compound **40** did not affect the body weight of the mice, suggesting that **40** was well tolerated *in vivo*. Additionally, western blotting and IHC results showed compound **40** decreased DPD expression in tumor and liver, and colon tissues from **40**-treated mice, consistent with our *in vitro* findings. Overall, our results demonstrated that the most potent compound **40** showed excellent reversion on 5-FU resistance *via* reducing DPD expression levels *in vitro* and *in vivo* and represents a promising lead candidate to treat 5-FU resistant colorectal cancer patients.

4. Experimental section

4.1. Chemical reagents and synthesis procedures

The analytical grade chemicals and solvents were gained from commercial companies. Unless otherwise stated, all commercial reagents were used without additional purification. If needs be, the solvents were purified and dried before use by standard methods. Dichloromethane (DCM) was dehydrated by CaH_2, and tetrahydrofuran (THF) was dried by sodium. Other solvents were dried by using the dried 4 Å molecular sieves. Thin-layer chromatography (TLC) was carried out by using silica gel plates (GF254) and visualization of chromatographic spots was affected at 254 nm and 365 nm. The crude compounds were purified by crystallization and column chromatography. ^{1}H NMR and ^{13}C NMR spectra were recorded in $CDCl_3$ or DMSO-d_6 at 400, 500 or 600 MHz on an Agilent spectrometer by using $CDCl_3$ as a reference standard (δ = 7.26 ppm) for ^{1}H NMR and (δ = 77.00 ppm) for ^{13}C NMR or DMSO-d_6 as a reference standard (δ = 2.50 ppm) for ^{1}H NMR and (δ = 39.52 ppm) for ^{13}C NMR. High-resolution mass spectra (HRMS) were recorded by using a Waters Xevo G2-XS QTOF spectrometer with an ESI ionization source. In addition, the Agilent 1290 Infinity HPLC and a reversed-phase C18 column (2.1 × 100 mm, 3.5 μm) were used to estimate the purity (>95 %) of the compounds. The compounds were dissolved in acetonitrile (1.5 mL), every sample was injected at a volume of 4 μL and eluted with a mixture of solvent acetonitrile and water (20/80, containing 0.1 % formic acid), the flow rate was 1 mL/min and the detection wavelength was 280 nm under UV.

4.1.1. Procedure for preparation of compounds ***10***, ***14***, ***18***

Compound **3** (1000 mg, 5.35 mmol) was mixed with $(CH_3)_2NH\cdot HCl$ (477 mg, 5.88 mmol), Et_3N (1081 mg, 10.70 mmol) in DCM (15 mL), and allowed to stir at room temperature for 8 h. Then the mixture was washed with water and extracted with DCM, the extract was combined and washed with saturated NaCl solution, dried over anhydrous $MgSO_4$, filtered, and concentrated *in vacuo*. The crude product was purified by column chromatography to afford the compound **4** (566 mg, 54 %) as a white solid. Compound **4** (500 mg, 2.55 mmol) was mixed with CH_3I (543 mg, 3.83 mmol), NaH (184 mg, 7.65 mmol) in dimethyl formamide (DMF, 15 mL) and allowed to stir under ice bath conditions for 2 h. Then the reaction was quenched with water and extracted with DCM, the extract was combined and washed with saturated NaCl solutions, then dried over anhydrous $MgSO_4$, filtered, and concentrated. The crude product was purified by column chromatography to afford the compound **5** (423 mg, 79 %) as a white solid. 80 % Hydrazine hydrate (3012 mg, 60.24 mmol) was mixed with a solution of **5** (229 mg, 1.09 mmol) in ethanol (10 mL). The mixture was heated at 100 °C for 3 h. Then the mixture was concentrated and washed with saturated NaCl solutions and extracted with DCM. The extract was dried over anhydrous MgSO4, filtered, and concentrated *in vacuo* to yield compound **6** as a white solid (204 mg, 91 %).

A mixture of 2,6-dichloroisonicotinic acid (1000 mg, 5.20 mmol), Et_3N (687 mg, 6.80 mmol), in 1,4-dioxane (10 mL) was allowed to stir at 0 °C and diphenyl phosphoryl azide (1900 mg, 6.80 mmol) was added dropwise. Then the mixture was warmed to room temperature. After the reaction was completed, the mixture was washed into 1 M $NaHCO_3$ solution and extracted with DCM. The extract was washed with saturated NaCl solution, dried over anhydrous $MgSO_4$, filtered, and concentrated *in vacuo*. The crude product was purified by column chromatography to afford compound **8** (753 mg, 67 %) as a white solid.

A solution of **8** (159 mg, 0.74 mmol) in toluene (1 mL) was refluxed for 2 h to produce the isocyanate **9**. The mixture was cooled to 50 °C, and compound **6** (152 mg, 0.74 mmol) in anhydrous THF (3 mL) was added, and the mixture was allowed to stir for another 8 h. Then the reaction mixture was concentrated *in vacuo*, and the residue was subjected to column chromatography to afford compound **10** (134 mg, 46 %) as a white solid.

Compound **14** was prepared from compound **6** through the similar procedure described for the synthesis of compound **10**.

Compound **6** (1000 mg, 5.35 mmol) was mixed with CH_3I (1140 mg, 8.03 mmol), NaH (385 mg, 16.05 mmol) in DMF (15 mL) and allowed to stir under an ice bath for 2 h the reaction mixture was quenched with water and extracted with DCM. The extract was combined and washed with saturated NaCl solutions, then dried over anhydrous $MgSO_4$, filtered, and concentrated *in vacuo*. The crude product was purified by column chromatography to afford the compound **15** (914 mg, 85 %) as a white solid. Compound **15** (900 mg, 4.48 mmol) was combined with Cs_2CO_3 (4378 mg, 13.43 mmol), $PdCl_2(PPh_3)_2$ (154 mg, 0.22 mmol), and 4-phenylboronic acid (547 mg, 4.48 mmol) in 1,4-dioxane/H_2O (20 mL, v/v 3/1). The mixture was degassed using two rounds of vacuum evacuation followed by nitrogen fill, then the mixture was allowed to stir at 80 °C for 12 h. After the reaction was completed, the mixture was washed with water and saturated NaCl solution, and extracted with DCM. The extract was dried over anhydrous $MgSO_4$, filtered, and concentrated *in vacuo*, the residue was subjected to column chromatography. Compound **16** was obtained as a white solid (533 mg, 49 %).

Compound **18** was prepared from **16** through the similar procedure described for the synthesis of compound **10**.

*2-Chloro-N,N-dimethyl-7H-pyrrolo[2,3-d]pyrimidin-4-amine (**4**).* White solid (54 %). ^{1}H NMR (500 MHz, DMSO-d_6) δ 11.76 (s, 1H), 7.10 (dd, J = 3.5, 2.4 Hz, 1H), 6.60 (dd, J = 3.6, 2.0 Hz, 1H). ^{13}C NMR (125 MHz, DMSO-d_6) δ 157.90, 152.47, 121.44, 102.50, 101.27, 39.14.

*2-Chloro-N,N,7-trimethyl-7H-pyrrolo[2,3-d]pyrimidin-4-amine (**5**).* White solid (79 %). ^{1}H NMR (500 MHz, DMSO-d_6) δ 7.08 (d, J = 3.6 Hz, 1H), 6.54 (d, J = 3.6 Hz, 1H), 3.62 (s, 3H), 3.21 (s, 6H). ^{13}C NMR (125 MHz, DMSO-d_6) δ 157.72, 152.50, 151.42, 125.40, 101.80, 101.32, 39.08, 31.48.

*2-Hydrazinyl-N,N,7-trimethyl-7H-pyrrolo[2,3-d]pyrimidin-4-amine (**6**).* White solid (92 %). ^{1}H NMR (500 MHz, DMSO-d_6) δ 7.00 (s, 1H), 6.76 (d, J = 3.6 Hz, 1H), 6.39 (d, J = 3.6 Hz, 1H), 3.55 (s, 3H), 3.20 (s, 6H). ^{13}C NMR (125 MHz, DMSO-d_6) δ 161.51, 157.81, 153.30, 121.71, 101.72, 96.96, 38.81, 31.01.

*N-(2,6-dichloropyridin-4-yl)-2-(4-(dimethylamino)-7-methyl-7H-pyrrolo[2,3-d]pyrimidin-2-yl)hydrazine-1-carboxamide (**10**).* White solid (46 %): mp 241.5–241.8 °C; ^{1}H NMR (500 MHz, DMSO-d_6) δ 9.58 (s, 1H), 8.44 (d, J = 97.7 Hz, 1H), 8.08 (s, 1H), 7.85 (s, 1H), 6.85 (d, J = 3.6 Hz, 1H), 6.45 (d, J = 3.6 Hz, 1H), 3.53 (s, 3H), 3.19 (s, 6H). ^{13}C NMR (125 MHz, DMSO-d_6) δ 159.16, 157.76, 152.87, 152.25, 149.71, 122.68, 111.66, 101.69, 98.27, 38.71, 31.05. HRESIMS *m/z* 417.0710 $[M+Na]^+$ (calcd for $C_{15}H_{16}Cl_2N_8ONa$ 417.0722).

*2,4-Dichloro-7-cyclopropyl-7H-pyrrolo[2,3-d]pyrimidine (**11**).* White solid (45 %). ^{1}H NMR (500 MHz, DMSO-d_6) δ 7.70 (d, J = 3.7 Hz, 1H), 6.62 (d, J = 3.7 Hz, 1H), 3.59 (td, J = 6.9, 3.5 Hz, 1H), 1.06 (dq, J = 7.9, 2.7 Hz, 4H). ^{13}C NMR (125 MHz, DMSO-d_6) δ 153.28, 151.31, 150.69, 132.59, 116.92, 99.17, 27.61, 6.49.

*4-(7-Cyclopropyl-2-hydrazinyl-7H-pyrrolo[2,3-d]pyrimidin-4-yl) morpholine (**13**).* White solid (95 %). ^{1}H NMR (500 MHz, DMSO-d_6) δ 7.18 (d, J = 3.7 Hz, 1H), 6.62 (d, J = 3.8 Hz, 1H), 3.80 (dd, J = 5.8, 4.0 Hz, 4H), 3.68 (dd, J = 5.8, 3.9 Hz, 4H), 3.51–3.45 (m, 1H), 1.02–0.91 (m, 4H). ^{13}C NMR (125 MHz, DMSO-d_6) δ 157.29, 153.36, 152.39, 124.71, 101.84, 101.21, 66.36, 45.85, 27.23, 6.43.

*2-(7-Cyclopropyl-4-morpholino-7H-pyrrolo[2,3-d]pyrimidin-2-yl)-N-(2,6-dichloropyridin-4-yl)hydrazine-1-carboxamide (**14**).* White solid (57 %): mp 241.4–241.9 °C; ^{1}H NMR (400 MHz, DMSO-d_6) δ 9.61 (s, 1H), 8.60 (s, 1H), 8.25 (s, 1H), 7.85 (s, 2H), 6.88 (s,

1H), 6.45 (d, J = 3.8 Hz, 1H), 3.76 (t, J = 4.7 Hz, 4H), 3.69–3.61 (m, 4H), 3.38 (q, J = 5.8 Hz, 1H), 0.90 (d, J = 5.0 Hz, 4H). ^{13}C NMR (100 MHz, DMSO-d_6) δ 159.03, 157.29, 154.74, 152.33, 149.77, 121.66, 111.71, 100.98, 67.49, 66.51, 45.84, 26.99, 6.39. HRESIMS *m/z* 463.1121 $[M+H]^+$ (calcd for $C_{19}H_{21}Cl_2N_8O_2$ 463.1165).

*2,4-Dichloro-7-methyl-7H-pyrrolo[2,3-d]pyrimidine (**15**).* White solid (85 %). ^{1}H NMR (500 MHz, DMSO-d_6) δ 7.71 (d, J = 3.6 Hz, 1H), 6.62 (d, J = 3.6 Hz, 1H), 3.78 (s, 3H). ^{13}C NMR (125 MHz, DMSO-d_6) δ 152.11, 151.26, 150.54, 133.75, 116.24, 99.15, 32.04.

*2-Chloro-7-methyl-4-phenyl-7H-pyrrolo[2,3-d]pyrimidine (**16**).* White solid (55 %). ^{1}H NMR (600 MHz, $CDCl_3$) δ 8.07 (dd, J = 7.7, 2.1 Hz, 2H), 7.52–7.48 (m, 3H), 7.16 (d, J = 3.6 Hz, 1H), 6.74 (d, J = 3.6 Hz, 1H), 3.83 (s, 3H). ^{13}C NMR (125 MHz, $CDCl_3$) δ 159.23, 153.61, 153.23, 136.97, 130.56, 129.01, 128.78, 114.40, 100.68, 31.46.

*N-(2,6-dichloropyridin-4-yl)-2-(7-methyl-4-phenyl-7H-pyrrolo [2,3-d]pyrimidin-2-yl)hydrazine-1-carboxamide (**18**).* White solid (39 %): mp 205.3–206.0 °C; ^{1}H NMR (400 MHz, DMSO-d_6) δ 9.72 (s, 1H), 8.82 (d, J = 43.4 Hz, 2H), 8.12 (d, J = 6.3 Hz, 2H), 7.89 (s, 1H), 7.55 (d, J = 6.7 Hz, 3H), 7.34 (s, 1H), 6.74 (s, 1H), 3.70 (s, 3H). ^{13}C NMR (100 MHz, DMSO-d_6) δ 159.83, 156.95, 154.03, 152.24, 149.85, 138.27, 130.53, 129.14, 128.89, 111.79, 100.09, 31.08. HRESIMS *m/z* 428.0711 $[M+H]^+$ (calcd for $C_{19}H_{16}Cl_2N_7O$ 428.0793).

4.1.2. Procedure for preparation of compounds **23a-23b, 25a-25b**

O-(mesitylsulfonyl)hydroxylamine (1000 mg, 4.65 mmol) was mixed with 2-(pyridine-2-yl)acetonitrile (549 mg, 4.65 mmol) in DCM (15 mL) and allowed to stir at room temperature for 1 h, then the reaction mixture was filtered to afford compound **21a** (465 mg, 30 %) as a white solid. Compound **21a** (400 mg, 1.20 mmol) and K_2CO_3 (332 mg, 2.40 mmol) were mixed in MeOH (10 mL) and allowed to stir at room temperature for 3 h. The mixture was washed with water and extracted with DCM, and the extract was washed with saturated NaCl solution, dried over anhydrous $MgSO_4$, filtered, and concentrated *in vacuo*. The crude product was purified by column chromatography to afford compound **22a** (64 mg, 40 %) as a white solid. Compound **23a** was prepared from **22a** through the similar procedure described for the synthesis of compound **10**, and compound **23b** was also prepared from compound **20b**.

Compound **22b** (300 mg, 1.42 mmol), Cs_2CO_3 (1391 mg, 4.27 mmol), $Pd(PPh_3)_4$ (819 mg, 0.71 mmol), and 4-phenylboronic acid (173 mg, 1.42 mmol) were added into 1,4-dioxane/H_2O (20 mL, v/v 3/1). The reaction mixture was degassed using two rounds of vacuum evacuation followed by nitrogen fill. The mixture was stirred at 80 °C for 3 h, and washed with water and saturated NaCl solution, and extracted with DCM. The extract was dried over anhydrous $MgSO_4$, filtered, and concentrated *in vacuo*, and the residue was subjected to column chromatography. Compound **24a** was obtained as a white solid (151 mg, 51 %). Compound **25a** was prepared from **24a** through the similar procedure described for the synthesis of compound **10**, and compounds **25b** was also prepared from compound **22b**.

Compound **21a-21b, 22a-22b** were obtained as described in the literature [31].

*1-(2,6-Dichloropyridin-4-yl)-3-(pyrazolo[1,5-a]pyridin-2-yl)urea (**23a**).* White solid (39 %): mp 241.8–242.2 °C; ^{1}H NMR (600 MHz, DMSO-d_6) δ 9.80 (s, 1H), 9.74 (s, 1H), 8.51 (d, J = 7.7 Hz, 1H), 7.58 (s, 2H), 7.53 (dt, J = 8.8, 1.1 Hz, 1H), 7.16 (ddd, J = 8.7, 6.7, 1.0 Hz, 1H), 6.78–6.75 (m, 1H), 6.62 (s, 1H). ^{13}C NMR (150 MHz, DMSO-d_6) δ 151.61, 151.41, 150.15, 149.75, 141.01, 128.69, 124.76, 117.43, 111.66, 111.58, 86.10. HRESIMS *m/z* 322.0260 $[M+H]^+$ (calcd for $C_{13}H_{10}Cl_2N_5O$ 322.0262).

*1-(6-Bromopyrazolo[1,5-a]pyridin-2-yl)-3-(2,6-dichloropyridin-4-yl)urea (**23b**).* White solid (46 %): mp 277.1–277.7 °C; ^{1}H NMR (600 MHz, DMSO-d_6) δ 9.93 (s, 1H), 9.82 (s, 1H), 8.90 (s, 1H), 7.57 (s, 2H), 7.54 (d, J = 9.4 Hz, 1H), 7.29 (dd, J = 9.3, 1.7 Hz, 1H), 6.68 (s, 1H). ^{13}C NMR (125 MHz, DMSO-d_6) δ 151.48, 151.24, 150.09, 150.05, 139.56, 128.73, 127.68, 118.33, 111.49, 104.84, 87.00. HRESIMS *m/z* 399.9362 $[M+H]^+$ (calcd for $C_{13}H_9Cl_2BrN_5O$ 399.9368).

*6-Phenylpyrazolo[1,5-a]pyridin-2-amine (**24a**).* White solid (51 %). ^{1}H NMR (600 MHz, DMSO-d_6) δ 8.55 (s, 1H), 7.64 (dd, J = 8.4, 1.1 Hz, 2H), 7.42–7.39 (m, 2H), 7.35–7.26 (m, 3H), 5.63 (s, 1H), 5.31 (s, 2H). ^{13}C NMR (150 MHz, DMSO-d_6) δ 129.51, 127.46, 126.46, 125.34, 123.43, 115.37, 81.85.

*1-(2,6-Dichloropyridin-4-yl)-3-(6-phenylpyrazolo[1,5-a]pyridin-2-yl)urea (**25a**).* White solid (42 %): mp 260.1–260.9 °C; ^{1}H NMR (600 MHz, DMSO-d_6) δ 9.89 (s, 1H), 9.81 (s, 1H), 8.86 (s, 1H), 7.72–7.70 (m, 2H), 7.64–7.62 (m, 1H), 7.59 (s, 2H), 7.54 (dd, J = 9.2, 1.6 Hz, 1H), 7.44 (t, J = 7.8 Hz, 2H), 7.34 (t, J = 7.4 Hz, 1H), 6.64 (s, 1H). ^{13}C NMR (125 MHz, DMSO-d_6) δ 151.49, 151.27, 150.16, 150.06, 139.95, 136.89, 129.49, 128.02, 126.85, 125.73, 124.67, 124.47, 117.43, 111.51, 86.08. HRESIMS *m/z* 398.0575 $[M+H]^+$ (calcd for $C_{19}H_{14}Cl_2N_5O$ 398.0575).

*6-(3-Methoxyphenyl)pyrazolo[1,5-a]pyridin-2-amine (**24b**).* White solid (59 %). ^{1}H NMR (600 MHz, DMSO-d_6) δ 8.58 (s, 1H), 7.35–7.28 (m, 3H), 7.20 (dt, J = 7.8, 1.2 Hz, 1H), 7.18–7.16 (m, 1H), 6.85 (dd, J = 8.0, 2.7 Hz, 1H), 5.62 (s, 1H), 5.31 (s, 2H), 3.78 (s, 3H). ^{13}C NMR (150 MHz, DMSO-d_6) δ 160.36, 159.65, 140.82, 139.11, 130.53, 125.53, 123.51, 118.77, 115.25, 113.22, 111.86, 81.88, 55.67.

*1-(2,6-Dichloropyridin-4-yl)-3-(6-(3-methoxyphenyl)pyrazolo [1,5-a]pyridin-2-yl)urea (**25b**).* White solid (57 %): mp 246.2–246.9 °C; ^{1}H NMR (500 MHz, DMSO-d_6) δ 9.90 (s, 1H), 9.83 (s, 1H), 8.92 (s, 1H), 7.66–7.60 (m, 3H), 7.57 (dd, J = 9.2, 1.7 Hz, 1H), 7.37 (t, J = 7.9 Hz, 1H), 7.31–7.27 (m, 2H), 6.93 (dd, J = 8.2, 1.7 Hz, 1H), 6.67 (s, 1H), 3.83 (s, 3H). ^{13}C NMR (100 MHz, DMSO-d_6) δ 160.32, 151.52, 151.31, 150.10, 140.05, 138.39, 130.57, 125.93, 124.59, 119.15, 117.36, 113.80, 112.29, 111.54, 86.13, 55.68. HRESIMS *m/z* 428.0673 $[M+H]^+$ (calcd for $C_{20}H_{16}Cl_2N_5O_2$ 428.0681).

4.1.3. Procedure for preparation of compounds **29, 33**

Cyanuric chloride (1000 mg, 5.47 mmol), pyrrole (388 mg, 5.47 mmol) were dissolved in acetone (10 mL) and the mixture was stirred at 0 °C for 5 h. Then the mixture was diluted with water and extracted with DCM. The extract was combined and washed with saturated NaCl solution, dried over anhydrous $MgSO_4$, filtered, and concentrated *in vacuo*. The crude product was purified by column chromatography to afford the compound **27** (620 mg, 52 %) as a white solid; Compound **27** (500 mg, 2.29 mmol) was mixed with phenylamine (213 mg, 2.29 mmol), Et_3N (462 mg, 4.58 mmol) in acetonitrile (10 mL) and stirred at 60 °C for 3 h. Then the mixture was poured into 1 M HCl solution, and extracted with DCM three times. The extract was combined and washed with water and saturated NaCl solutions, dried over anhydrous $MgSO_4$, filtered, and concentrated *in vacuo* to yield a crude product. Then the crude product was purified by column chromatography to afford compound **27** (378 mg, 60 %) as a white solid. 80 % Hydrazine hydrate (3012 mg, 60.24 mmol) was mixed with a solution of **27** (300 mg, 1.09 mmol) in ethanol (10 mL). The mixture was heated at 100 °C for 3 h. Then the mixture was concentrated and washed with saturated NaCl solutions and extracted with DCM. The extract was dried over anhydrous $MgSO_4$, filtered, and concentrated *in vacuo* to yield compound **28** as a white solid (269 mg, 91 %).

A solution of **8** (159 mg, 0.74 mmol) in toluene (1 mL) was refluxed for 2 h to produce the isocyanate **9**. The mixture was cooled to 50 °C, and compound **28** (200 mg, 0.74 mmol) in anhydrous THF (3 mL) was added, and the mixture was allowed to stir for another 8 h. Then the reaction mixture was concentrated *in vacuo*, and the residue was subjected to column chromatography to afford compound 2**9** (187 mg, 55 %) as a white solid.

Compounds **33** were prepared through a similar procedure from compounds **30**.

*4-Chloro-N-phenyl-6-(pyrrolidin-1-yl)-1,3,5-triazin-2-amine (**27**).* White solid (60 %). ^{1}H NMR (500 MHz, DMSO-d_6) δ 9.98 (s, 1H), 7.72 (s, 2H), 7.28 (t, J = 7.8 Hz, 2H), 7.03–6.96 (m, 1H), 3.48 (dt, J = 30.2, 6.2 Hz, 4H), 1.95–1.82 (m, 4H). ^{13}C NMR (125 MHz, DMSO-d_6) δ 162.89, 139.50, 128.99, 123.14, 120.24, 46.93, 46.71, 25.10, 24.96.

*2,6-Dichloroisonicotinoyl azide (**28**).* White solid (67 %). ^{1}H NMR (500 MHz, DMSO-d_6) δ 7.88 (s, 2H). ^{13}C NMR (125 MHz, DMSO-d_6) δ 169.37, 150.92, 143.78, 122.71.

*N-(2,6-dichloropyridin-4-yl)-2-(4-(phenylamino)-6-(pyrrolidin-1-yl)-1,3,5-triazin-2-yl)hydrazine-1-carboxamide (**29**).* White solid (55 %): mp 243.6–243.9 °C; ^{1}H NMR (400 MHz, DMSO-d_6) δ 9.72 (d, J = 95.6 Hz, 1H), 9.16 (s, 1H), 8.72 (s, 2H), 7.99–7.47 (m, 4H), 7.06 (d, J = 131.0 Hz, 3H), 3.49 (s, 4H), 1.90 (s, 4H). ^{13}C NMR (150 MHz, DMSO-d_6) δ 164.45, 163.76, 152.21, 140.95, 130.17, 128.78, 128.63, 121.87, 120.05, 111.88, 46.52, 46.34, 31.82, 29.56, 29.24, 29.11, 25.32, 22.63, 14.50. HRESIMS m/z 460.1149 $[M+H]^+$ (calcd for $C_{19}H_{20}Cl_2N_9O$ 460.1168).

*2-Chloro-N,6-dimethylpyrimidin-4-amine (**31**).* White solid (33 %). ^{1}H NMR (600 MHz, $CDCl_3$) δ 6.35 (s, 1H), 6.07 (s, 1H), 2.92 (d, J = 4.6 Hz, 3H), 2.31 (s, 3H). ^{13}C NMR (150 MHz, $CDCl_3$) δ 165.06, 160.08, 159.99, 98.34, 29.76, 28.52, 23.92.

*2-Hydrazinyl-N,6-dimethylpyrimidin-4-amine (**32**).* White solid (95 %). ^{1}H NMR (600 MHz, DMSO-d_6) δ 7.26 (s, 1H), 6.68 (s, 1H), 5.56 (s, 1H), 3.96 (s, 2H), 2.69 (d, J = 4.2 Hz, 3H), 2.02 (s, 3H). ^{13}C NMR (150 MHz, $CDCl_3$) δ 169.63, 169.08, 32.24, 28.77.

*N-(2,6-dichloropyridin-4-yl)-2-(4-methyl-6-(methylamino)pyrimidin-2-yl)hydrazine-1-carboxamide (**33**).* White solid (51 %): mp 214.0–214.2 °C; ^{1}H NMR (500 MHz, DMSO-d_6) δ 9.53 (s, 1H), 8.58 (s, 1H), 8.19 (s, 1H), 7.68 (d, J = 168.2 Hz, 2H), 6.92 (s, 1H), 5.76 (s, 1H), 2.68 (s, 3H), 2.05 (s, 3H). ^{13}C NMR (125 MHz, DMSO-d_6) δ 164.39, 163.37, 152.18, 149.75, 111.69, 23.90. HRESIMS m/z 342.0465 $[M+H]^+$ (calcd for $C_{12}H_{14}Cl_2N_7O$ 342.0637).

4.1.4. Procedure for preparation of compounds **34–40**

Compounds **34–40** were prepared from acid azide **7** and different amines through the similar procedure described for the synthesis of compound **10**.

*1-(2,6-Dichloropyridin-4-yl)-3-(2,6-dimethylpyridin-4-yl)urea (**34**).* White solid (59 %): mp 209.9–210.6 °C; ^{1}H NMR (400 MHz, DMSO-d_6) δ 9.74 (s, 1H), 9.48–9.36 (m, 1H), 7.55 (s, 2H), 7.14 (s, 2H), 2.37 (s, 6H). ^{13}C NMR (100 MHz, DMSO-d_6) δ 158.12, 151.87, 151.23, 150.08, 146.86, 111.52, 109.58, 24.47. HRESIMS m/z 311.0468 $[M+H]^+$ (calcd for $C_{13}H_{13}Cl_2N_4O$ 311.0466).

*1-(3,5-Dichlorophenyl)-3-(2,6-dichloropyridin-4-yl)urea (**35**).* White solid (49 %): mp 243.8–244.9 °C; ^{1}H NMR (400 MHz, DMSO-d_6) δ 9.58 (d, J = 72.3 Hz, 2H), 7.55–7.50 (m, 4H), 7.18 (t, J = 1.9 Hz, 1H). ^{13}C NMR (100 MHz, DMSO-d_6) δ 151.91, 151.26, 150.04, 141.61, 134.59, 122.42, 117.47, 111.56. HRESIMS m/z 349.9423 $[M+H]^+$ (calcd for $C_{12}H_8Cl_4N_3O$ 349.9421).

*N-(2,6-Dichloropyridin-4-yl)-4-methylpiperazine-1-carboxamide (**36**).* White solid (44 %): mp 105.3–106.4 °C; ^{1}H NMR (400 MHz, DMSO-d_6) δ 9.38 (d, J = 4.5 Hz, 1H), 7.61 (t, J = 4.0 Hz, 2H), 3.47 (q, J = 4.8 Hz, 4H), 2.33 (q, J = 4.7 Hz, 4H), 2.21 (d, J = 4.5 Hz, 3H). ^{13}C NMR (100 MHz, DMSO-d_6) δ 153.73, 152.72, 149.70, 111.72, 54.73, 46.08, 44.16. HRESIMS m/z 371.0673 $[M+H]^+$ (calcd for $C_{15}H_{17}Cl_3N_4O_2$ 371.0678).

*1-(2,6-Dichloropyridin-4-yl)-3-(1,3-dimethyl-1H-pyrazol-5-yl) urea (**37**).* White solid (67 %): mp 168.3–169.6 °C; ^{1}H NMR (400 MHz, DMSO-d_6) δ 9.73 (s, 1H), 8.96 (s, 1H), 7.55 (s, 2H), 5.98 (s, 1H), 3.59 (s, 3H), 2.10 (s, 3H). ^{13}C NMR (100 MHz, DMSO-d_6) δ 151.76, 151.48, 150.04, 145.92, 136.63, 111.40, 98.62, 35.32, 14.10. HRESIMS m/z 300.0423 $[M+H]^+$ (calcd for $C_{11}H_{12}Cl_2N_5O$ 300.0419).

*1-(2-Chloropyridin-4-yl)-3-(2,6-dichloropyridin-4-yl)urea (**38**).* White solid (56 %): mp 200.6–201.5 °C; ^{1}H NMR (400 MHz, DMSO-d_6) δ 9.79 (s, 2H), 8.23 (d, J = 5.6 Hz, 1H), 7.64 (d, J = 1.8 Hz, 1H), 7.55 (s, 2H), 7.37 (dd, J = 5.6, 1.9 Hz, 1H). ^{13}C NMR (100 MHz, DMSO-d_6) δ 151.71, 151.45, 150.94, 150.53, 150.08, 148.68, 112.77, 112.39, 111.72. HRESIMS m/z 316.9763 $[M+H]^+$ (calcd for $C_{11}H_8Cl_3N_4O$ 316.9764).

*1-(3,5-Dichloro-4-methoxyphenyl)-3-(2,6-dichloropyridin-4-yl) urea (**39**)*: mp 237–237.5 °C; White solid (49 %). ^{1}H NMR (400 MHz, DMSO-d_6) δ 9.74 (s, 1H), 9.37 (s, 1H), 7.57 (d, J = 15.0 Hz, 4H), 3.79 (s, 3H). ^{13}C NMR (100 MHz, DMSO-d_6) δ 152.04, 151.43, 150.04, 147.24, 136.46, 128.62, 119.66, 111.56, 61.12. HRESIMS m/z 379.9524 $[M+H]^+$ (calcd for $C_{13}H_{10}Cl_4N_3O_2$ 379.9527).

*1,3-Bis(2,6-dichloropyridin-4-yl)urea (**40**).* White solid (55 %): mp 245.3–246.1 °C; ^{1}H NMR (400 MHz, DMSO-d_6) δ 9.97 (s, 2H), 7.55 (s, 4H). ^{13}C NMR (100 MHz, DMSO-d_6) δ 151.63, 150.84, 150.12, 111.93. HRESIMS m/z 350.9372 $[M+H]^+$ (calcd for $C_{11}H_7Cl_4N_4O$ 350.9374).

4.1.5. Procedure for preparation of compounds **44a-44d**

A mixture of 2,6-dichloroisonicotinic acid (1000 mg, 5.24 mmol) in methanol (15 mL) was stirred at room temperature and 1 M NaOH (7 mL) was added dropwise, then the mixture was heated at 70 °C for 8 h. The pH value of the reaction mixture was adjusted to 5. The mixture was washed with water, and extracted with DCM, and the extract was washed with saturated NaCl solution, dried over anhydrous $MgSO_4$, filtered, and concentrated *in vacuo*. The crude product was purified by column chromatography to afford compound **41a** (636 mg, 65 %) as a white solid. The acid azide **42a** was prepared from compound **41a** through the similar procedure of compound **7.** Then compound **44a** was prepared through a similar procedure to compound **10**, and compounds **44a-44d** were also prepared from compound **6**.

*2-Chloro-6-methoxyisonicotinic acid (**41a**).* White solid (65 %). ^{1}H NMR (400 MHz, DMSO-d_6) δ 13.97 (s, 1H), 7.40 (d, J = 1.0 Hz, 1H), 7.19 (d, J = 1.0 Hz, 1H), 3.91 (s, 3H). ^{13}C NMR (100 MHz, DMSO-d_6) δ 165.09, 164.51, 148.56, 144.77, 115.99, 109.78, 54.96.

*2-Chloro-6-ethoxyisonicotinic acid (**41b**).* White solid (82 %). ^{1}H NMR (400 MHz, DMSO-d_6) δ 13.94 (s, 1H), 7.38 (d, J = 1.0 Hz, 1H), 7.14 (d, J = 1.0 Hz, 1H), 4.33 (q, J = 7.0 Hz, 2H), 1.33 (t, J = 7.0 Hz, 3H). ^{13}C NMR (100 MHz, DMSO-d_6) δ 165.11, 164.10, 148.53, 144.74, 115.81, 109.83, 63.37, 14.65.

*2-Chloro-6-isopropoxyisonicotinic acid (**41c**).* White solid (85 %). ^{1}H NMR (400 MHz, DMSO-d_6) δ 13.89 (s, 1H), 7.34 (d, J = 1.0 Hz, 1H), 7.08 (d, J = 1.0 Hz, 1H), 5.18 (h, J = 6.2 Hz, 1H), 1.30 (d, J = 6.2 Hz, 6H). ^{13}C NMR (100 MHz, DMSO-d_6) δ 165.10, 163.62, 148.49, 144.75, 115.53, 110.28, 70.15, 21.99.

*2-Chloro-6-(cyclopentyloxy)isonicotinic acid (**41d**).* White solid (60 %). ^{1}H NMR (400 MHz, DMSO-d_6) δ 13.86 (s, 1H), 7.33 (d, J = 1.0 Hz, 1H), 7.08 (d, J = 1.0 Hz, 1H), 5.29 (td, J = 5.9, 3.0 Hz, 1H), 2.04–1.83 (m, 2H), 1.78–1.51 (m, 6H). ^{13}C NMR (100 MHz, DMSO-d_6) δ 165.09, 163.80, 148.50, 144.61, 115.54, 110.18, 79.56, 32.57, 23.82.

*2-Chloro-6-methoxyisonicotinoyl azide (**42a**).* White solid (58 %). ^{1}H NMR (400 MHz, DMSO-d_6) δ 7.41 (d, J = 1.1 Hz, 1H), 7.20 (d, J = 1.1 Hz, 1H), 3.92 (s, 3H). ^{13}C NMR (100 MHz, DMSO-d_6) δ 170.24, 164.59, 149.02, 143.43, 115.11, 109.39, 55.17.

*2-Chloro-6-ethoxyisonicotinoyl azide (**42b**).* White solid (50 %). ^{1}H NMR (400 MHz, $CDCl_3$) δ 7.39 (d, J = 1.1 Hz, 1H), 7.18 (d, J = 1.1 Hz, 1H), 4.39 (q, J = 7.1 Hz, 2H), 1.40 (t, J = 7.1 Hz, 3H). ^{13}C NMR (100 MHz, $CDCl_3$) δ 170.37, 164.24, 149.64, 142.38, 114.80, 109.39, 63.36, 14.32.

*2-Chloro-6-isopropoxyisonicotinoyl azide (**42c**).* White solid (81 %). ^{1}H NMR (400 MHz, $CDCl_3$) δ 7.36 (d, J = 1.2 Hz, 1H), 7.13 (d, J = 1.2 Hz, 1H), 5.31 (p, J = 6.2 Hz, 1H), 1.36 (d, J = 6.1 Hz, 6H). ^{13}C NMR (100 MHz, $CDCl_3$) δ 170.38, 163.80, 149.56, 142.33, 114.43, 109.84, 70.15, 21.74.

*2-Chloro-6-(cyclopentyloxy)isonicotinoyl azide (**42d**).* White solid (79 %). ^{1}H NMR (400 MHz, $CDCl_3$) δ 7.35 (d, J = 1.2 Hz, 1H), 7.13 (d,

J = 1.2 Hz, 1H), 5.41 (tt, J = 6.1, 2.9 Hz, 1H), 2.06–1.91 (m, 2H), 1.85–1.73 (m, 4H), 1.71–1.58 (m, 2H). ^{13}C NMR (100 MHz, $CDCl_3$) δ 170.38, 164.01, 149.59, 142.23, 114.42, 109.69, 79.75, 32.62, 23.82.

*1-(2-Chloro-6-methoxypyridin-4-yl)-3-(2,6-dichloropyridin-4-yl) urea (**44a**).* White solid (59 %): mp 229.7–230.9 °C; ^{1}H NMR (400 MHz, DMSO-d_6) δ 10.03 (s, 2H), 7.55 (s, 2H), 7.18 (d, J = 1.5 Hz, 1H), 6.89 (d, J = 1.5 Hz, 1H), 3.83 (s, 3H). ^{13}C NMR (100 MHz, DMSO-d_6) δ 164.59, 151.97, 151.32, 150.65, 150.08, 148.34, 111.74, 106.76, 96.87, 54.36. HRESIMS *m/z* 346.9868 $[M+H]^+$ (calcd for $C_{12}H_{10}Cl_3N_4O_2$ 346.9869).

*1-(2-Chloro-6-ethoxypyridin-4-yl)-3-(2,6-dichloropyridin-4-yl) urea (**44b**).* White solid (37 %): mp 223.5–224.1 °C; ^{1}H NMR (400 MHz, DMSO-d_6) δ 9.74 (d, J = 50.9 Hz, 2H), 7.54 (s, 2H), 7.16 (d, J = 1.5 Hz, 1H), 6.82 (d, J = 1.4 Hz, 1H), 4.24 (q, J = 7.0 Hz, 2H), 1.30 (t, J = 7.0 Hz, 3H). ^{13}C NMR (100 MHz, DMSO-d_6) δ 164.17, 151.70, 151.04, 150.49, 150.09, 148.32, 111.74, 106.63, 97.10, 62.57, 14.80. HRESIMS *m/z* 361.0024 $[M+H]^+$ (calcd for $C_{13}H_{12}Cl_3N_4O_2$ 361.0026).

*1-(2-Chloro-6-methoxypyridin-4-yl)-3-(2,6-dichloropyridin-4-yl) urea (**44c**).* White solid (64 %): mp 108.4–109.4 °C; ^{1}H NMR (400 MHz, DMSO-d_6) δ 9.81 (s, 2H), 7.55 (s, 2H), 7.16 (d, J = 1.5 Hz, 1H), 6.79 (d, J = 1.5 Hz, 1H), 5.12 (hept, J = 6.1 Hz, 1H), 1.28 (d, J = 6.2 Hz, 6H). ^{13}C NMR (100 MHz) δ 111.79, 40.62, 40.41, 40.20, 39.99, 39.78, 39.57, 39.37, 22.20. HRESIMS *m/z* 375.0180 $[M+H]^+$ (calcd for $C_{14}H_{14}Cl_3N_4O_2$ 375.0182).

*1-(2-Chloro-6-(cyclopentyloxy)pyridin-4-yl)-3-(2,6-dichloropyridin-4-yl)urea (**44d**).* White solid (48 %): mp 117.8–118.3 °C; ^{1}H NMR (400 MHz, DMSO-d_6) δ 9.67 (d, J = 63.3 Hz, 2H), 7.47 (s, 2H), 7.06 (s, 1H), 6.74 (s, 1H), 5.17 (tt, J = 5.7, 2.6 Hz, 1H), 1.92–1.75 (m, 2H), 1.73–1.45 (m, 6H). ^{13}C NMR (100 MHz, DMSO-d_6) δ 163.91, 151.70, 151.05, 150.43, 150.08, 148.30, 111.71, 106.40, 97.54, 78.68, 32.69, 23.83. HRESIMS *m/z* 401.0338 $[M+H]^+$ (calcd for $C_{16}H_{16}Cl_3N_4O_2$ 401.0339).

4.2. Cell culture

Colorectal cancer cell lines HCT116, SW620, and normal colonic epithelial cell line NCM460 were gained from Shanghai Cell Bank, Chinese Academy of Science (Shanghai, China) and were cultured in Dulbecco's Modified Eagle's Medium (DMEM) or RPMI 1640 medium which contained 10 % FBS, 50 IU penicillin and 50 mg/mL streptomycin. The condition of cell culture is at 37 °C in a humid incubator with 5 % CO_2. The resistant HCT116^{DPD} cells were obtained as previous study and resistant SW620/5-FU cells were gained through continual treatment of 5-FU.

4.3. Antiproliferative activity in vitro

Cell viability was routinely assessed by 3-[4,5-dimethylthiazol-2-yl]-2,5-diphenyl tetrazolium bromide (MTT) assay. Logarithmic growth phase cells were cultured in the 96-well plates at a concentration of 3 × 10^3 cells/mL. 20 μL serum-containing media (5 mg/mL) with MTT reagent was added in cell cultures and incubate for 4 h at 37 °C and analyzed by the microplate reader by the 490 nm wave. The cells were cultured with 20 μM 5-FU and compounds for 48 h, and the experiment was repeated three times. The growth inhibition rate was calculated as follows: Inhibition rate = 1- (OD_{Drug} - OD_{Blank})/($OD_{Control}$ - OD_{Blank}). The values of EC_{50} (20 μM 5-FU plus compound) and IC_{50} (compound) were calculated from the dose-response curves of the assays (Prism 7.0).

4.4. Western blotting analysis

Quantify the cell or tissue lysates by the BCA assay according to the standard curve. Then separate the proteins by SDS-PAGE and vertically transfer them to the PVDF membrane. After the block of 5 % BSA for 90 min, the membranes were incubated with the primary antibody of DPD (Abcam, ab180609) and β-actin (Sigma-Aldrich, A5441) in 1 % BSA/PBS containing Tween-20 (TBST) 4 °C overnight. Afterward, all membranes were rinsed with TBST (3 × 10 min) and cultured with the corresponding secondary antibody at 37 °C for 1 h, extensively washed with TBST for 3 × 10 min, enhanced signals on the membranes were detected by ECL chemiluminescent detection system and quantified by the ratio of density value.

4.5. HPLC analysis of intracellular 5-FU and FBAL

Concentrations of intracellular 5-FU and FBAL were determined by HPLC-UV analysis. Both 5-FU and FBAL standards (0.2, 1, 5, 10, 25, 50 mg/L) were used to calculate the corresponding standard curves. Treated with 25 mg/L 5-FU plus 2 μM compound **40** or 2 μM JTE-013 to culture with 6 h, cell lysates were sonicated in the ice-water bath for 30 min and vortex mixed for 30 s. Then centrifuge the cell lysates at 2000 g for 10 min at 4 °C, and load the supernatant into the solid-phase styrene-divinylbenzene resin column. Evaporate the elutes for dryness and dissolve them into the methanol. HPLC-UV was then taken to compare and quantify the 5-FU and FBAL levels of each group, as described previously [32].

4.6. Binding kinetics assay

The affinity of compounds towards S1PR2 protein was determined using SPR assays on a GE BiacoreT200 (GE, USA). S1PR2 protein was immobilized on a CM5 chip (GE, USA) by amine coupling procedures achieving a RU of 15000 and activated with sterile buffer (EDC/NHS, 1/1) with a flow rate of 30 μL/min for 15 min, and the chip immobilized S1PR2 was sealed with ethanolamine for 8 min. The test compounds were dissolved in DMSO and diluted with purified water, and the association of serial dilutions of the compounds was performed at 25 °C with PBSP buffer solution (1 % DMSO) with a flow rate of 30 μL/min for 60 s, whereas dissociation of the compounds from the S1PR2 was determined for 60s. The kinetic parameters were calculated by the BiacoreT200 SPR evaluation software. All sinograms were fitted using a kinetic fitting model provided by the BiacoreT200 SPR evaluation software, and the association (K_a) and dissociation (K_d) rate constants were used to calculate the equilibrium dissociation constants (K_D).

4.7. 3D computational modeling and molecule docking

Molecular docking was initiated from the construction of the model of S1PR2, which was from the crystal complex of S1PR1 (PDB code: 3V2Y). Molecular docking simulations in the S1PR2 were run using the LeDock due to its high accuracy in pose prediction and very fast speed. Ligands were prepared with the ChemBio3D Ultra 14.0, followed by MM2 energy minimization. Protein structures were also prepared with the LePro, which could automatically add hydrogen atoms to proteins by explicitly considering the protonation state of histidine. After this step, the orthosteric binding site was gained from the known crystal complex of S1PR1 and its ligand. The allosteric binding site was deduced as described in the literature [30]. The ligands were docked to the S1PR2 using LeDock through flexible docking mode. Top scoring function poses were selected as representative of the simulations and were displayed with PyMOL software.

4.8. Pharmacokinetic profile

All animal care and experimental procedures were performed in

accordance with the regulations for animal experimentation issued by Institute Animal Care and Welfare Committee, and approved by the Institutional Animal Care and Use Committee at Ocean University of China. Sprague-Dawley rats (adult male) weighing 180–220 g were obtained from Ji'nan Pengyue Laboratory Animal Breeding Co., Ltd. (approval number: SCXK 20190003). The rats were acclimated for seven days prior to the study on a 12 h light/12 h dark cycle at 22 ± 2 °C, 60 % relative humidity. They were allowed free access to water and a chow diet. Rats were given **40** (1.0 mg/kg) or JTE-013 (1.0 mg/kg) through the tail vein. The dosing solutions were prepared by dissolving in solvent consists of 1% DMSO, 4 % polyoxyethylene castor Oil, and 95 % distilled water. Blood samples (350 μL) were collected into heparinized ice-bathed polythene tubes via the retrobulbar plexus bleeding under isoflurane anesthesia before dosing and at 2, 5, 15, and 30 min and 1, 2, 4, 6, 8, 12, and 24 h after intravenous administration. Immediately after collection, a 100 μL aliquot of blood was removed from each sample, and the remaining heparinized whole blood was processed to plasma by centrifugation at 1660*g* for 5 min. Blood and plasma samples were stored at −40 °C until analysis.

All samples (100 μL) were added to an internal standard (IS, JTE-013 when analyzing **40, 40** when analyzing JTE-013, final concentration 100 ng/mL, respectively) and 200 μL ice-bathed acetonitrile. All mixtures were vortexed and centrifuged at 17968 g for 10 min twice at 4 °C to precipitate protein. A 5 μL aliquot of each supernatant was then injected into the LC-MS/MS system for analysis.

4.9. In vitro incubation assays

Mice liver microsomes (MLMs) and rats liver microsomes (RLMs) with a final protein concentration of 0.5 mg/mL were pre-incubated with an NADPH-regenerating system (containing 0.011 mol/L β-nicotinamide adenine dinucleotide phosphate, 0.110 mol/L glucose 6-phosphate, and 10 U/mL glucose-6-phosphate dehydrogenase) in 50 mmol/L Tris-HCl buffer (pH 7.4) at 37 °C for 5 min. Then, **40** was added at a final concentration of 2 μmol/L to initiate the reaction. All samples were placed in 37 °C for incubation and were quenched with two volumes of acetonitrile with IS (final concentration 200 ng/mL) at 60 min and then vortex-mixed and centrifuged at 18,880 g for 10 min. The supernatant was subjected to LC–MS/MS analysis. The results were expressed as the percentage of the concentration at 0 min.

4.10. LC-MS/MS analysis

LC-MS/MS instrument (Thermo Fisher Scientific, Waltham, MA, USA) consisted of a DIODEX UltiMate 3000 UHPLC system and TSQ Quantiva triple quadrupole mass spectrometer with Xcalibur 2.2 software for data acquisition and processing. **40** and JTE-13 were chromatographed using an Eclipse Plus C18 column (3.5 μm, 2.1 × 50 mm, Agilent, Santa Clara, CA, USA) at 30 °C.

The mobile phase consisted of solvent A (0.1 % formic acid in water) and solvent B (0.1 % formic acid in acetonitrile). Separation was performed at a flow rate of 0.2 mL/min with the following gradient elution: 0.0–1.5 min, 20 % solvent B; 1.5–1.6 min, a linear gradient runs from 20 % to 80 % solvent B; 1.6–3.5 min, 80 % solvent B; 3.5–3.6 min, a linear gradient runs from 80 % to 20 % solvent B; 3.6–5.0 min 20 % solvent B for re-equilibration. A H-ESI source was used in the positive ion mode. The detection was operated in selective reaction monitoring (SRM) with a dwell time of 100 ms for each transition. The transition of **40** and JTE-013 were *m/z* 350.84 → 188.89 (collision energy: 18.6 V, RF lens: 189.7) and *m/z* 408.17 → 203.06 (collision energy: 22.3 V, RF lens: 94.5), respectively. The mass spectrometric condition was optimized as follows: ion spray voltage, 4000 V; ion transfer tube temperature, 325 °C; vaporizer temperature, 275 °C; sheath gas, nitrogen, 30 arb; aux gas, nitrogen, 20 arb; sweep gas, nitrogen, 0.8 arb; collision gas, argon, 2.0 mTorr.

4.11. Data analysis

Pharmacokinetic parameters, based on plasma and whole blood concentrations, were calculated by classical noncompartmental analysis via WinNonlin Software (version 6.3, Pharsight Corporation, Mountain View, CA, USA).

4.12. Determination of the effect of compound **40** to reverse 5-FU resistance in vivo

2×10^6/mL SW620/5-FU cells were subcutaneously inoculated into the left or right flanks of athymic nude mice. When the tumor volume of each group reached approximately 150–200 mm^3, all mice were randomly divided into 5 groups (n = 6), which were all consecutively treated by tail vein injection for 24 days. Compound **40**, JTE-013, and 5-FU were respectively administrated at the dose of 1.08 mg/kg, 12.5 mg/kg, and 20 mg/kg. The solvent consists of 30 % PEG300, 5 % Tween 80, 2 % DMSO, and 63 % distilled water. Tumor volumes and mice health conditions were daily recorded. On day 24, each group of mice was sacrificed and liver, colon, and tumoral tissues were all collected and fixed for further western blotting and histological analysis. All animal experiments were approved by the Animal Welfare Committee of Capital Medical University for scientific purposes (permit no. AEEI-2016-043).

4.13. Immunohistochemistry analysis

Multiple tissue samples were all fixed in 4 % formaldehyde solution and embedded in paraffin on 4 μm thick sections. After the blocking step, the slides were incubated with the primary antibody of DPD (Abcam, ab180609) at 4 °C overnight. Besides, all slides were also incubated with the IgG isotype as the control. We used an axioplan microscope to observe DAB staining and scanned the slides by KF-PRO-OO5 slide viewer, which were then visually inspected by two observers to avoid subjective bias. IHC scoring was obtained based on the staining intensity and percentage of stained cancer cells as previously described [33].

Author's contribution

Shengbiao Wan and Xianjun Qu conceived and designed the study. Dongdong Luo, Xiaochen Tian, Yan Lv designed and synthesized all compounds, and the animals and cellular experiments were performed by Yuhang Zhang, Shuang Yang, Zhikun Guo, Xiaochun Liu, Gaitian Han, Shuai Liu and Wenyu Wang. Dongdong Luo, Yuhang Zhang, and Shuang Yang wrote the manuscript, and all authors edited it.

Declaration of competing interest

The authors declare that they have no known competing financial interests or personal relationships that could have appeared to influence the work reported in this paper.

Acknowledgments

We are grateful for the support of the National Natural Science Foundation of China (81973170, 91629303, 81673449, 81872884, 81973350); NSFC-Shandong Joint Fund for Marine Science Research Centers (U1606403), and Beijing Natural Science Foundation and

Scientific Research Program of Municipal Commission of Education (KZ201710025020, KZ201810025033).

Abbreviations used

5-FU	5-Fluorouracil
CRC	colorectal cancer
S1PR2	sphingosine-1-phosphate receptor 2
FBAL	α-fluoro-β-alanine
DPD	dihydropyrimidine dehydrogenase
GPCRs	G-protein-coupled receptors
COX-2	cyclooxygenase-2
PG	prostaglandin
FUTP	5-fluorouridine-5′-triphosphate
FdUTP	5-fluoro-2′-deoxyuridine-5′-triphosphate
FdUMP	5-fluoro-2′-deoxyuridine-5′-monophosphate
TS	thymidylate synthase
DHFU	5,6-dihydro-5-fluorouracil
CDHP	gimeracil
S1P	sphingosine-1-phosphate
SPR	surface plasmon resonance
ER	endoplasmic reticulum
TLC	thin-layer chromatography
HRMS	high-resolution mass spectra

Appendix A. Supplementary data

Supplementary data to this article can be found online at https://doi.org/10.1016/j.ejmech.2021.113775.

References

[1] M.G. Fakih, Metastatic colorectal cancer: current state and future directions, J. Clin. Oncol. 33 (2015) 1809–1824.
[2] R.L. Siegel, K.D. Miller, S.A. Fedewa, D.J. Ahnen, R.G.S. Meester, A. Barzi, A. Jemal, Colorectal cancer statistics, CA A Cancer J. Clin. 67 (2017) (2017) 177–193.
[3] F. Bray, J. Ferlay, I. Soerjomataram, R.L. Siegel, L.A. Torre, A. Jemal, Global cancer statistics 2018: GLOBOCAN estimates of incidence and mortality worldwide for 36 cancers in 185 countries, CA A Cancer J. Clin. 68 (2018) 394–424.
[4] D. Salonga, K.D. Danenberg, M. Johnson, R. Metzger, S. Groshen, D.D. Tsao-Wei, H.J. Lenz, C.G. Leichman, L. Leichman, R.B. Diasio, P.V. Danenberg, Colorectal tumors responding to 5-fluorouracil have low gene expression levels of dihydropyrimidine dehydrogenase, thymidylate synthase, and thymidine phosphorylase, Clin. Canc. Res. 6 (2000) 1322–1327.
[5] D.B. Longley, D.P. Harkin, P.G. Johnston, 5-fluorouracil: mechanisms of action and clinical strategies, Nat. Rev. Canc. 3 (2003) 330–338.
[6] W.A. Hammond, A. Swaika, K. Mody, Pharmacologic resistance in colorectal cancer: a review, Ther. Adv. Med. Oncol. 8 (2016) 57–84.
[7] M.M. Gottesman, T. Fojo, S.E. Bates, Multidrug resistance in cancer: role of ATP-dependent transporters, Nat. Rev. Canc. 2 (2002) 48–58.
[8] D.B. Longley, P.G. Johnston, Molecular mechanisms of drug resistance, J. Pathol. 205 (2005) 275–292.
[9] G. Szakacs, J.K. Paterson, J.A. Ludwig, C. Booth-Genthe, M.M. Gottesman, Targeting multidrug resistance in cancer, Nat. Rev. Drug Discov. 5 (2006) 219–234.
[10] M. Gerlinger, A.J. Rowan, S. Horswell, M. Math, J. Larkin, D. Endesfelder, E. Gronroos, P. Martinez, N. Matthews, A. Stewart, P. Tarpey, I. Varela, B. Phillimore, S. Begum, N.Q. McDonald, A. Butler, D. Jones, K. Raine, C. Latimer, C.R. Santos, M. Nohadani, A.C. Eklund, B. Spencer-Dene, G. Clark, L. Pickering, G. Stamp, M. Gore, Z. Szallasi, J. Downward, P.A. Futreal, C. Swanton, Intratumor heterogeneity and branched evolution revealed by multiregion sequencing, N. Engl. J. Med. 366 (2012) 883–892.
[11] R.A. Gatenby, R.J. Gillies, J.S. Brown, Evolutionary dynamics of cancer prevention, Nat. Rev. Canc. 10 (2010) 526–527.
[12] L.X. Qiu, Q.Y. Tang, J.L. Bai, X.P. Qian, R.T. Li, B.R. Liu, M.H. Zheng, Predictive value of thymidylate synthase expression in advanced colorectal cancer patients receiving fluoropyrimidine-based chemotherapy: evidence from 24 studies, Int. J. Canc. 123 (2008) 2384–2389.
[13] K.J. Sohn, R. Croxford, Z. Yates, M. Lucock, Y.I. Kim, Effect of the methylenetetrahydrofolate reductase C677T polymorphism on chemosensitivity of colon and breast cancer cells to 5-fluorouracil and methotrexate, J. Natl. Cancer Inst. 96 (2004) 134–144.
[14] M. Panczyk, Pharmacogenetics research on chemotherapy resistance in colorectal cancer over the last 20 years, World J. Gastroenterol. 20 (2014) 9775–9827.
[15] R. Soong, N. Shah, M. Salto-Tellez, B.C. Tai, R.A. Soo, H.C. Han, S.S. Ng, W.L. Tan, N. Zeps, D. Joseph, R.B. Diasio, B. Iacopetta, Prognostic significance of thymidylate synthase, dihydropyrimidine dehydrogenase and thymidine phosphorylase protein expression in colorectal cancer patients treated with or without 5-fluorouracil-based chemotherapy, Ann. Oncol. 19 (2008) 915–919.
[16] F. Innocenti, R. Danesi, G. Bocci, G. Natale, M. Del Tacca, 5-Fluorouracil catabolism to 5-fluoro-5,6-dihydrouracil is reduced by acute liver impairment in mice, Toxicol. Appl. Pharmacol. 203 (2005) 106–113.
[17] A.B. van Kuilenburg, J. Haasjes, D.J. Richel, L. Zoetekouw, H. Van Lenthe, R.A. De Abreu, J.G. Maring, P. Vreken, A.H. van Gennip, Clinical implications of dihydropyrimidine dehydrogenase (DPD) deficiency in patients with severe 5-fluorouracil-associated toxicity: identification of new mutations in the DPD gene, Clin. Canc. Res. 6 (2000) 4705–4712.
[18] M. Scartozzi, E. Maccaroni, R. Giampieri, M. Pistelli, A. Bittoni, M. Del Prete, R. Berardi, S. Cascinu, 5-Fluorouracil pharmacogenomics: still rocking after all these years? Pharmacogenomics 12 (2011) 251–265.
[19] M.C. van Staveren, F. Opdam, H.J. Guchelaar, A.B. van Kuilenburg, J.G. Maring, H. Gelderblom, Influence of metastatic disease on the usefulness of uracil pharmacokinetics as a screening tool for DPD activity in colorectal cancer patients, Canc. Chemother. Pharmacol. 76 (2015) 47–52.
[20] T. Ochiai, M. Umeki, H. Miyake, T. Iida, M. Okumura, K. Ohno, M. Sakamoto, N. Miyoshi, M. Takahashi, H. Tsumura, Y. Tokunaga, H. Naitou, T. Fukui, Impact of 5-fluorouracil metabolizing enzymes on chemotherapy in patients with resectable colorectal cancer, Oncol. Rep. 32 (2014) 887–892.
[21] K. Hirata, N. Horikoshi, K. Aiba, M. Okazaki, R. Denno, K. Sasaki, Y. Nakano, H. Ishizuka, Y. Yamada, S. Uno, T. Taguchi, T. Shirasaka, Pharmacokinetic study of S-1, a novel oral fluorouracil antitumor drug, Clin. Canc. Res. 5 (1999) 2000–2005.
[22] T. Takechi, A. Fujioka, E. Matsushima, M. Fukushima, Enhancement of the antitumour activity of 5-fluorouracil (5-FU) by inhibiting dihydropyrimidine dehydrogenase activity (DPD) using 5-chloro-2,4-dihydroxypyridine (CDHP) in human tumour cells, Eur. J. Canc. 38 (2002) 1271–1277.
[23] Y.H. Zhang, D.D. Luo, S.B. Wan, X.J. Qu, S1PR2 inhibitors potently reverse 5-FU resistance by downregulating DPD expression in colorectal cancer, Pharmacol. Res. 155 (2020), 104717.
[24] X. Yue, H. Jin, H. Liu, A.J. Rosenberg, R.S. Klein, Z. Tu, A potent and selective C-11 labeled PET tracer for imaging sphingosine-1-phosphate receptor 2 in the CNS demonstrates sexually dimorphic expression, Org. Biomol. Chem. 13 (2015) 7928–7939.
[25] K. Kusumi, K. Shinozaki, Y. Yamaura, A. Hashimoto, H. Kurata, A. Naganawa, K. Otsuki, T. Matsushita, T. Sekiguchi, A. Kakuuchi, H. Yamamoto, T. Seko, Discovery of novel S1P2 antagonists, part 3: improving the oral bioavailability of a series of 1,3-bis(aryloxy)benzene derivatives, Bioorg. Med. Chem. Lett 26 (2016) 1209–1213.
[26] K. Kusumi, K. Shinozaki, Y. Yamaura, A. Hashimoto, H. Kurata, A. Naganawa, H. Ueda, K. Otsuki, T. Matsushita, T. Sekiguchi, A. Kakuuchi, T. Seko, Discovery of novel S1P2 antagonists. Part 2: improving the profile of a series of 1,3-bis(aryloxy)benzene derivatives, Bioorg. Med. Chem. Lett 25 (2015) 4387–4392.
[27] K. Kusumi, K. Shinozaki, T. Kanaji, H. Kurata, A. Naganawa, K. Otsuki, T. Matsushita, T. Sekiguchi, A. Kakuuchi, T. Seko, Discovery of novel S1P2 antagonists. Part 1: discovery of 1,3-bis(aryloxy)benzene derivatives, Bioorg. Med. Chem. Lett 25 (2015) 1479–1482.
[28] Z. Luo, X. Yue, H. Yang, H. Liu, R.S. Klein, Z. Tu, Design and synthesis of pyrazolopyridine derivatives as sphingosine 1-phosphate receptor 2 ligands, Bioorg. Med. Chem. Lett 28 (2018) 488–496.
[29] Z. Luo, H. Liu, R.S. Klein, Z. Tu, Design, synthesis, and in vitro bioactivity evaluation of fluorine-containing analogues for sphingosine-1-phosphate 2 receptor, Bioorg. Med. Chem. 27 (2019) 3619–3631.
[30] H. Satsu, M.T. Schaeffer, M. Guerrero, A. Saldana, C. Eberhart, P. Hodder, C. Cayanan, S. Schurer, B. Bhhatarai, E. Roberts, H. Rosen, S.J. Brown, A sphingosine 1-phosphate receptor 2 selective allosteric agonist, Bioorg. Med. Chem. 21 (2013) 5373–5382.
[31] Y. Nishigaya, K. Umei, E. Yamamoto, Y. Kohno, S. Seto, Direct access to 2-aminopyrazolo[1,5-a]pyridines via N-amination/cyclization reactions of 2-pyridineacetonitriles, Tetrahedron Lett. 55 (2014) 5963–5966.
[32] J.H. Liu, T.H. Tsai, Y.J. Chen, L.Y. Wang, H.Y. Liu, C.H. Hsieh, Local irradiation modulates the pharmacokinetics of metabolites in 5-fluorouracil-radiotherapy-pharmacokinetics phenomenon, Front. Pharmacol. 11 (2020) 141.
[33] C. Sun, R. Zargham, Q. Shao, X. Gui, V. Marcus, A. Lazaris, A. Salman, P. Metrakos, X. Qu, Z. Gao, Association of CD98, integrin beta1, integrin beta3 and Fak with the progression and liver metastases of colorectal cancer, Pathol. Res. Pract. 210 (2014) 668–674.